© 2007 The Chemical Society of Japan

Award Accounts

The Chemical Society of Japan Award for 2005

Studies on Two- and Three-Dimensional π-Conjugated Systems with Unique Structures and Properties

Koichi Komatsu

Department of Environmental and Biotechnological Frontier Engineering, Fukui University of Technology, 3-6-1 Gakuen, Fukui 910-8505

Received May 24, 2007; E-mail: komatsu@fukui-ut.ac.jp

A series of two-dimensional, cyclic π-conjugated systems with the six-membered to eight-membered rings as well as polycyclic aromatic compounds and sulfur-containing compounds, which were fully surrounded by rigid bicyclic σ-frameworks, were synthesized and their structures and properties elucidated. This structural modification is characteristic to cause an elevation of the HOMO levels of neutral π-systems and to stabilize remarkably the corresponding cationic systems by both thermodynamic and kinetic effects. In contrast to annelation with a strain-free bicyclic system, such as bicyclo[2.2.2]octene, annelation with a more strained system, such as bicyclo[2.1.1]hexene, brings about a large bond fixation effect upon the cyclic π-system. Thus, π-conjugated systems with quite unusual electronic structures can be prepared by using combination of these structural modifications. As another example of unusual structure, a novel three-dimensional π-conjugated system, i.e., fullerene encapsulating molecular hydrogen, was synthesized from empty fullerene using organic reactions. This is taken as an entirely new approach to the endohedral fullerenes, of which the production has so far relied only on physical methods.

Introduction

Chemistry of π-conjugated systems is important not only as the fundamental science,[1] but for better understanding the performance of functional organic molecules.[2] Among a wide variety of π-conjugated systems known, those which are the subject in Section **1** of this article are confined to cyclic π-conjugated systems made of mostly hydrocarbons (and some others containing sulfur atoms). Particularly, the focus is placed on species with unusual or non-natural electronic structures.

Various methods to control the properties of two-dimensional π-conjugated systems have been reported. These include the manipulation of the size and shape of π-conjugated systems and/or introduction of n–π conjugative heteroatom(s) either as a member of the ring system or as the substituent(s). In Section **1**, the author will describe how we can utilize σ-frameworks surrounding the π-systems to control the properties of the two-dimensional π-conjugated systems, without relying on such a method as the use of heteroatom(s).[3,4]

Whereas π-conjugation is most effective in one- or two-dimensional systems, three-dimensional systems, such as bowl-shaped[5,6] or twisted systems,[7] have been the subject of theoretical interest, and from this, there appeared molecules with an ultimate π-conjugated geometry in the field of three-dimensional system, that is, the fullerenes.[8,9] In Section **2** of this article, some particular types of reactions of fullerene, C_{60}, will be described, which led us to the first synthesis of endohedral fullerene encapsulating molecular hydrogen.

1. Cyclic π-Conjugated Systems Surrounded by Polycycloalkene Frameworks

When σ-bonds are rigidly fixed at the position nearly parallel to the 2p orbitals of π-conjugated systems, there should appear an electronic interaction between the σ- and π-orbitals, that is, σ–π interaction or C–C hyperconjugation. In general, the energy levels of σ and π molecular orbitals are widely separated so that the electronic interaction between them is considered to be quite small. However, when the geometrical fixation of these σ-bonds is rigid and if the number of such σ-bonds is maximal, accumulative effects could become significant. For the purpose of rigidly fixing the σ-bonds in the right position, annelation of the π-system with polycycloalkene frameworks was found to be satisfactory as will be shown.

1.1 Benzenoid Aromatic Hydrocarbons Annelated with Bicyclo[2.2.2]octene. Among possible polycycloalkenes to be annelated to the cyclic π-systems, we first selected bicyclo[2.2.2]octene (abbreviated as BCO throughout this article), because it does not impose much angle strain on the π-system and furnishes σ-bonds rigidly fixed at the right position for σ–π interaction. As the most basic cyclic π-conjugated systems, benzene **1**,[10] naphthalene **2**,[11] anthracene **3**,[12] and fluorene **4**[13] were synthesized. Also, benzyne **5** annelated with two BCO groups was generated in solution. In the absence of any catalyst it underwent dimerization to give biphenylene **6**,[14] whereas it underwent cyclotrimerization to give triphenylene **7**[15] in the presence of a Pd catalyst (Chart 1).

Published on the web December 13, 2007; doi:10.1246/bcsj.80.2285

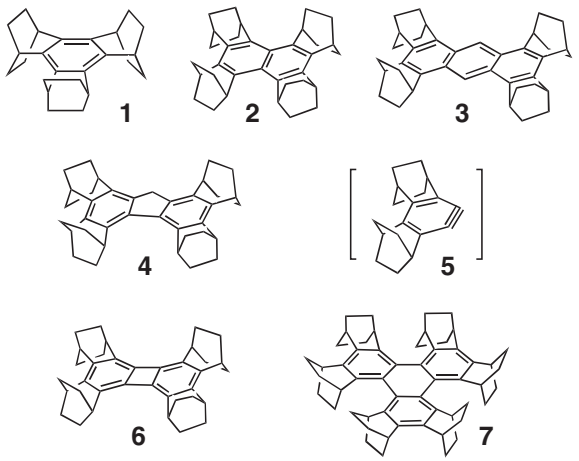

Chart 1.

Table 1. Oxidation Potentials (V vs. Fc/Fc^+)[a] for BCO-Annelated Benzenoid Compounds, **1**, **2**, **3**, **4**, **6**, and **7**

Compd	$E_{1/2}$ (1)[b]	E_{pa} (2)[c]	Ref.
1	+1.08	—	17
2	+0.33	+1.17	17
3	+0.17	+0.86	17
4	+0.56	+0.88	13
6	+0.25	+1.00	17
7	+0.44	+1.27	15

a) In $CHCl_2CHCl_2$ with 0.1 M Bu_4NClO_4; scan rate 20 $mV\,s^{-1}$. b) Reversible wave. c) Irreversible peak.

All of these benzenoid hydrocarbons **1**–**7** were characterized by well-defined reversible oxidation waves in cyclic voltammogram (CV) at remarkably low potentials, resulting from the elevation of the HOMO due to σ–π interaction. The values of oxidation potential are shown in Table 1. Most of the condensed aromatics also underwent a second oxidation to the dications. In agreement with the results of electrochemistry, these aromatic hydrocarbons were transformed into stable radical cations in solution with characteristic coloration[16] upon oxidation with $SbCl_5$ in CH_2Cl_2.

It should be emphasized here that most of the salts of these hydrocarbon radical cations ($\mathbf{2}^{\bullet+}$, $\mathbf{3}^{\bullet+}$, $\mathbf{4}^{\bullet+}$, and $\mathbf{6}^{\bullet+}$) are isolable as single crystals, thus allowing detailed structural analysis by X-ray crystallography (Fig. 1).[17] In the case of radical cation salt of triphenylene **7**, it slowly underwent rearrangement to a stable arenium ion $\mathbf{8}^+$, of which the structure was also determined by X-ray crystallography.[15] Triphenylene **7** can not take a planar structure because of steric congestion between the BCO units. The release of this strain is assumed to be the driving force for this rearrangement (Scheme 1).

The change in π-bond lengths upon one-electron oxidation of **2**, **3**, **4**, and **6** is systematically related to the coefficients of the relevant carbons in HOMOs of the neutral molecules. The π-bonds with bonding nature in the HOMO are elongated upon removal of one electron, and those with antibonding nature in HOMO are shortened.

In addition, there is a tendency of characteristic changes in the σ-bond lengths of the bicyclic frameworks in radical cations $\mathbf{2}^{\bullet+}$, $\mathbf{3}^{\bullet+}$, $\mathbf{4}^{\bullet+}$, and $\mathbf{6}^{\bullet+}$ (Scheme 2). Although the extent

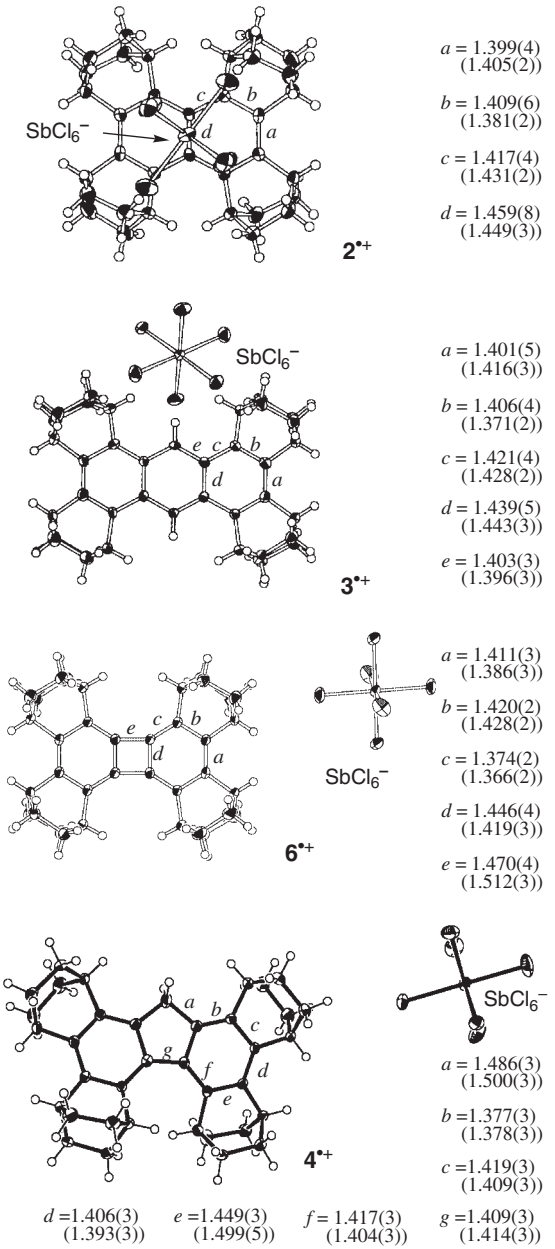

Fig. 1. The X-ray crystal structures of radical cation salts, $\mathbf{2}^{\bullet+}SbCl_6^-$, $\mathbf{3}^{\bullet+}SbCl_6^-$, $\mathbf{6}^{\bullet+}SbCl_6^-$, and $\mathbf{4}^{\bullet+}SbCl_6^-$, together with the values of bond lengths (Å); values in parentheses are those for neutral compounds.

is quite small, the C_{Ar}–C_α bonds (*a* and *b*) (antibonding in the HOMO of the neutral molecules) appear to be shortened, whereas all of the C_α–C_β bonds (*c* and *d*) (bonding in the HOMO) are elongated, compared to those of the corresponding neutral molecules. These changes in σ-bond lengths can be taken as experimental evidence for the presence of σ–π conjugation (C–C hyperconjugation) to stabilize these radical cations.[17,18]

As has been shown by CV, naphthalene **2**, anthracene **3**, fluorene **4**, and biphenylene **6**, underwent two-electron oxidation to the corresponding dications by using an excess amount of SbF_5 in CD_2Cl_2 under vacuum. The dications were characterized by ^1H and ^{13}C NMR.[13,14,17] The ^1H NMR signals for

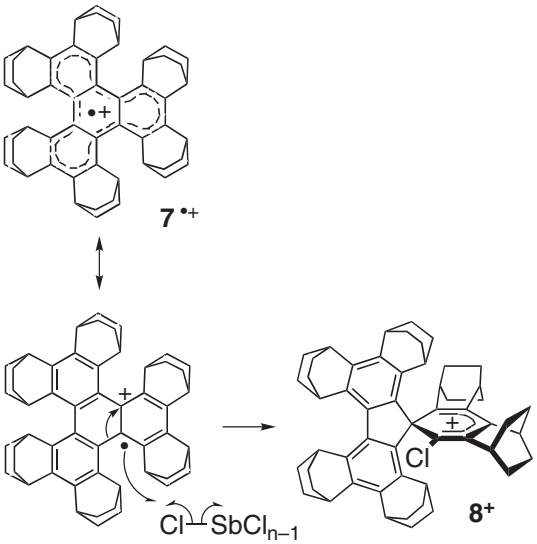

Scheme 1.

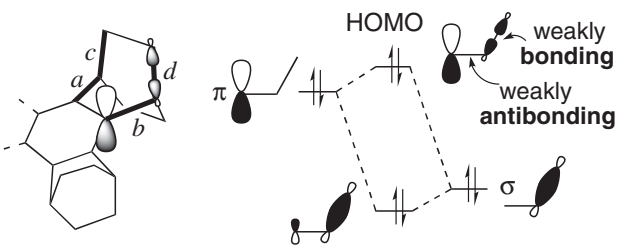

Scheme 2.

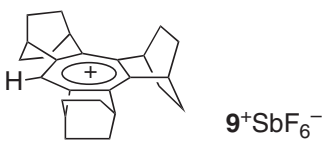

Chart 2.

the BCO units' bridgehead protons located in the same plane as the π-systems shifted upfield for **2** (10π-electron) and **3** (14π-electron) upon going from the neutral compounds to dications, reflecting the change from an aromatic $(4n+2)\pi$ system to an antiaromatic $4n\pi$ system. Accordingly, the reverse tendency was observed for 12π-electron system **6**.

1.2 Tropylium and Silatropylium Ions Annelated with Bicyclo[2.2.2]octene. As shown above, the positively charged π-systems are effectively stabilized by annelation of the BCO units. We utilized this method to synthesize tropylium ion **9**$^+$ (Chart 2) with extraordinary stability by annelation with three BCO units.[19] The cation **9**$^+$ has the pK_{R^+} value of 13.0 (25 °C in 50% aqueous MeCN) and can be only half-neutralized in 0.1 M NaOH.

The remarkable thermodynamic stability of tropylium ion **9**$^+$ led us to try for the synthesis of the first silylium cation with the silicon incorporated in a carbonaceous π-conjugated system, silatropylium ion **11**$^+$. Theoretical calculations indicate that, in contrast to the case of trimethylsilyl cation (Mulliken charge +0.89 on Si), the Mulliken charge on Si is +0.56 and the rest of charge is delocalized over the rest of the π-system in the parent silatropylium ion. Furthermore,

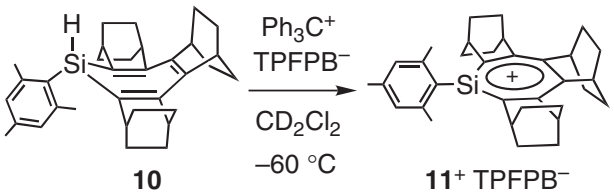

Scheme 3.

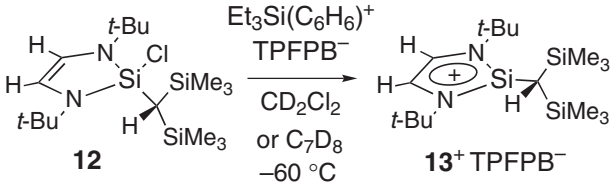

Scheme 4.

the system is aromatic to a certain extent as estimated from calculated values of nucleus independent chemical shift at 1 Å above the ring (NICS(1); silatropylium ion −7.3, tropylium ion −10.7)[20] and magnetic susceptibility exaltation (MSE; silatropylium ion −15.6, tropylium ion −20.1).[20]

When one equivalent of triphenylmethyl tetrakis(pentafluorophenyl)borate (Ph$_3$C$^+$TPFPB$^-$) was added to a solution of silepin **10** in CD_2Cl_2 at −60 °C, the ^{1}H NMR spectrum indicated quantitative formation of tris-BCO-annelated silatropylium ion **11**$^+$ (Scheme 3).[20] The Si–H proton (δ 4.81) in **10** disappeared and was replaced by Ph$_3$C–H proton (δ 5.55). The most noteworthy are the 0.6–0.9 ppm downfield shifts of BCO's bridgehead protons (δ 3.70, 3.65, and 3.22) as compared with those of silepin **10** (δ 2.78 (4H) and 2.59 (2H)), providing experimental proof for the presence of aromatic ring current in this silatropylium ion. The ^{29}Si NMR signal was observed at 142.9 ppm, which is shifted downfield by 192.2 ppm compared to precursor silepin **10** (−49.3 ppm). The ^{13}C NMR signals for the seven-membered ring carbons (175.9, 153.2, and 149.7 ppm) are also shifted downfield compared to **10** (152.0, 145.5, and 141.8 ppm), indicating considerable positive-charge delocalization in the seven-membered ring.[20]

This result also prompted us to investigate another π-conjugated silylium cation, i.e., silaimidazolium ion **13**$^+$. As the precursor, chlorosilane **12** having a bulky bis(trimethylsilyl)-methyl (Dis) group on the silicon atom was chosen, and it was treated with 1 equivalent of [Et$_3$Si(benzene)]$^+$TPFPB$^-$ in CD_2Cl_2 or in toluene-d_8 under vacuum at −60 °C (Scheme 4). Generation of 2-silaimidazolium ion **13**$^+$ was clearly demonstrated by ^{29}Si NMR spectroscopy.[21] A set of signals was observed at 53.0 and 4.3 ppm in CD_2Cl_2 and at 53.2 and 4.0 ppm in toluene-d_8. The signal at the lower field was assigned to that for the cationic silicon based on the peak intensity as well as the fact that it was in fair agreement with the estimated value, 60.0 ppm, by GIAO calculation at B3LYP/6-311+G(2df,p)//B3LYP/6-31G(d) level. This signal is 70 ppm downfield shifted from that of precursor **12**. The signal of the methine proton in the Dis group in **13**$^+$ was observed at 1.39 ppm, which is 1.06 ppm downfield shifted compared to that in **12**. In the optimized structure of **13**$^+$, the methine proton is positioned almost on the plane of the 2-silaimidazolium ring, and therefore the proton nucleus is strongly affected by a

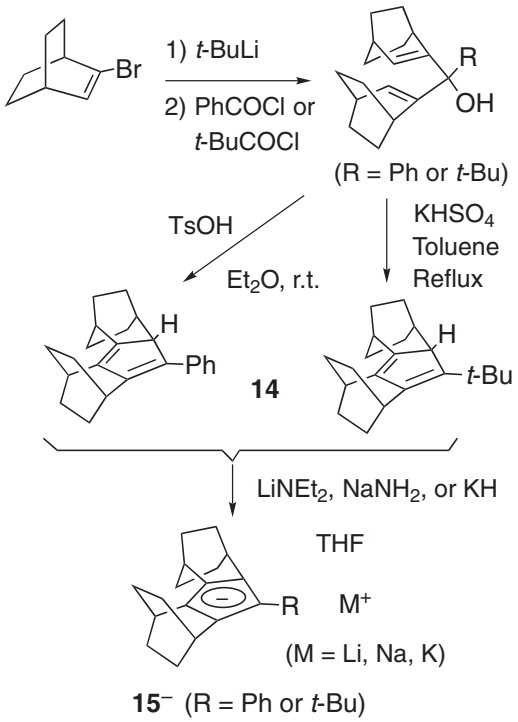

Scheme 5.

diamagnetic ring current. This suggests the presence of 6π aromaticity in the 2-silaimidazolium ring. The NICS value calculated for a model compound, 1,2,3-trimethyl-2-silaimidazolium, and its carbon analogue, 1,2,3-trimethylimidazolium, was -6.5 and -10.9 ppm, respectively, thus supporting the presence of aromaticity in **13**$^+$ to some extent.[21]

1.3 Cyclopentadienyl System Annelated with Bicyclo[2.2.2]octene. What can we expect when we prepare a cyclopentadienyl π-system annelated with BCO units? Since the internal angle of a pentagon is relatively small (108°), annelation with BCO units is anticipated to cause considerable angle strain on the π-system. However, we could successfully synthesize cyclopentadienes **14** (R = Ph, *t*-Bu) (Scheme 5), which were converted to the corresponding cyclopentadienide anions **15**$^-$ by treating with $LiNEt_2$, $NaNH_2$, or KH in THF-d_8.[22] Among these, X-ray crystallography was conducted for Li^+ and Na^+ salts of **15**$^-$ (R = Ph) and Na^+ salt of **15**$^-$ (R = *t*-Bu), as shown for the last salt in Fig. 2. As shown, these salts constitute contact ion-pair with three molecules of THF complexed to the metal ion. Unfortunately, it was not possible to convert the anions into the corresponding radicals or cations. However, annelation of the π-system with BCO units was found to be advantageous in that one face of the π-system, on which a chemical event takes place, can be distinguished from the other by observing the ^{13}C NMR signals of the BCO's methylene carbons.

For example, broad two singlets for the BCO's two methylene carbons of the Li^+ salt of **15**$^-$ (R = Ph) underwent gradual line broadening and then splitting into four singlets as the temperature was lowered from 40 °C down to −60 °C as shown in Fig. 3 together with simulated spectra. This represents the dynamic behavior of the Li^+**15**$^-$ salt. Since the externally added LiBr salt did not affect the line-shape, this behavior is considered to be due to an internal exchange of the site of Li^+ complexation by the **15**$^-$ (R = Ph) ion. Thus, the metal ion is considered to exchange positions between the upper and lower faces of the cyclopentadienyl (Cp) ring (Scheme 6). Similar behavior was observed for all of the **15**$^-$ salts.[22] From a detailed study of the concentration dependence of the dynamic behavior, the metal-ion exchange was found to proceed principally as an intramolecular process at concentration

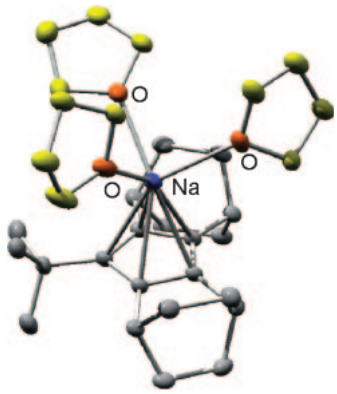

Fig. 2. X-ray crystal structure of Na^+**15**$^{-\bullet}$(thf)$_3$ (R = *t*-Bu).

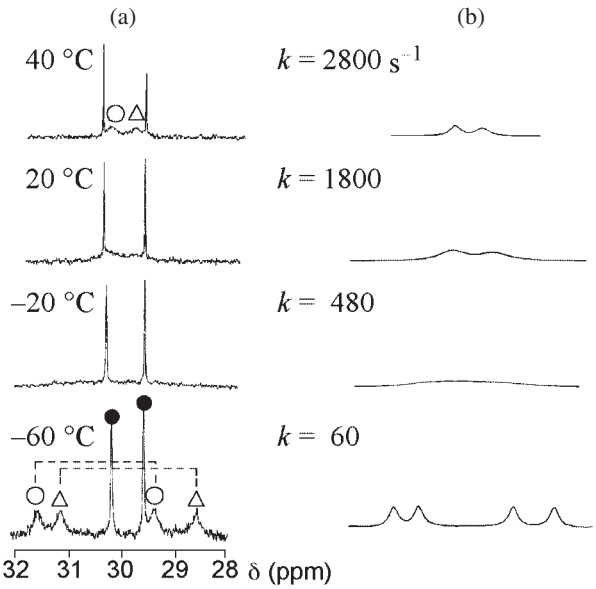

Fig. 3. Temperature-dependent (a) experimental and (b) simulated ^{13}C NMR spectra of Li^+**15**$^-$ (R = Ph) in THF-d_8. The signals marked with ○ and △ correspond to methylene carbons and those marked with ● corresponds to bridgehead carbons of the BCO units. [Li^+**15**$^-$] = 0.1 M.

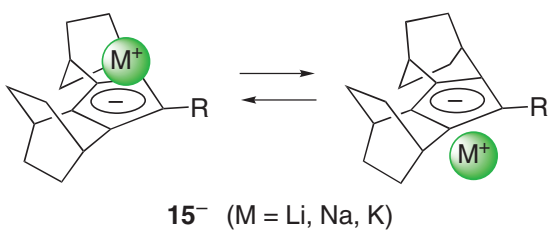

Scheme 6.

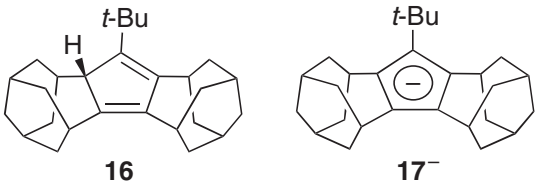

Chart 3.

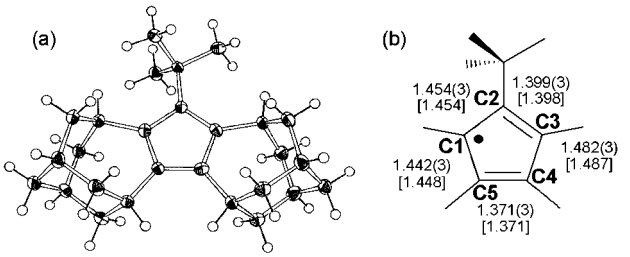

Fig. 4. (a) Molecular structure of **17•** determined by X-ray crystallography. (b) Selected bond distances (Å). Values from fully optimized UB3LYP/6-31G* are given in square brackets.

ranges lower than 0.2 M. The experimentally obtained $\Delta G^{\neq}$ values for the intramolecular exchange process for all M^+**15**$^-$ salts (except for Li^+**15**$^-$ (R = *t*-Bu), of which the intramolecular process was too slow to observe) were found to be quite similar in THF-d_8 and to be within the range of 12–14 kcal mol^{-1}. Within this range, the $\Delta G^{\neq}$ value was found to increase as the size of the metal ion decreased.[22]

1.4 Cyclopentadienyl System Annelated with Homoadamantene Units. Homoadamantene (abbreviated as HAd) is a system that can also rigidly hold sigma bonds in an arrangement nearly parallel to the 2p orbitals. Because the inner angles of the olefinic carbon are wider than those in bicyclo[2.2.2]octene, annelation of a Cp ring with HAd does not impose much strain on the system. Thus, *t*-butylcyclopentadiene annelated with two HAd units **16** was synthesized in the similar manner to the one used for the synthesis of **14**.

The corresponding Cp anion **17**$^-$ was readily obtained by deprotonation of **16** using KC_8 or KH in THF (Chart 3). One-electron oxidation of anion **17**$^-$ afforded the Cp radical **17•** as air-sensitive yellow crystals.[23] Prior to this work, there was an X-ray crystal study on fully π-conjugated penta(isopropyl)-Cp radical with an effective hyperconjugative stabilization by isopropyl groups.[24] In sharp contrast to the case of $(i\text{-Pr})_5Cp^{\bullet}$, in which the spin is completely delocalized, the X-ray crystallography analysis of *t*-Bu$(HAd)_2$Cp radical (**17•**) indicated a clear bond alternation and localization of the spin as shown in Fig. 4. The molecule has a C_s symmetry plane passing through the planar Cp ring. The bond lengths of C2–C3 and C4–C5 are similar to or only slightly longer (by 0.047 and 0.037 Å respectively) than the corresponding double bonds in neutral Cp **16**, whereas other C–C bonds have lengths typical of C(sp^2)–C(sp^2) single bonds. One of the C–CH_3 bonds of the *t*-Bu group is oriented antiperiplanar to the radical center, with the other two methyl carbons positioned above and below the Cp-ring plane. The position of the radical center is controlled by the conformation of the *t*-Bu group, the rotational barrier of which is calculated to be only 2.6 kcal mol^{-1}.[23]

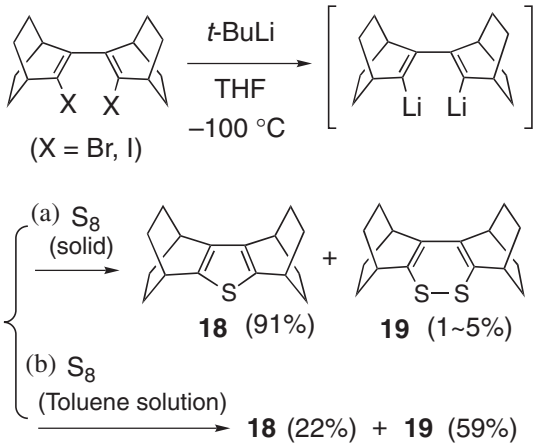

Scheme 7.

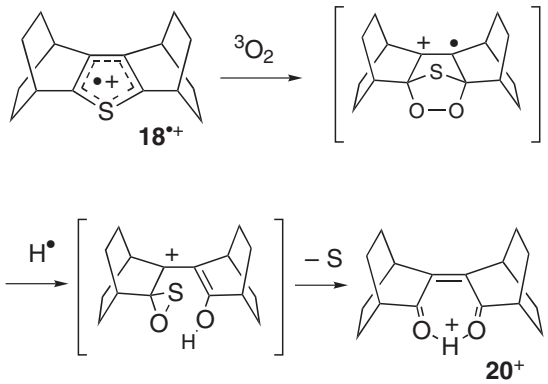

Scheme 8.

1.5 Sulfur-Containing Systems Annelated with Bicyclo-[2.2.2]octene. 1.5.1 Thiophene Annelated with Bicyclo-[2.2.2]octene: Thiophene is a 6π aromatic, sulfur-containing π-system isoelectronic to benzene. Its bis-BCO annelated derivative **18** was synthesized, together with 1,2-dithiin **19** (see below) from the dihalide of BCO dimer as shown in Scheme 7a.[25] In the CV of **18**, a well-defined reversible oxidation wave was observed at +0.79 V vs. Fc/Fc^+ in CH_2Cl_2, in contrast to the irreversible oxidation waves observed for peralkylated thiophene derivatives.[26] Chemical one-electron oxidation of thiophene **18** with 1.5 equivalents of either $SbCl_5$ or SbF_5 in CH_2Cl_2 gave a yellow solution, which exhibited a persistent five-line ESR signal (a_H = 0.346 mT, g = 2.00215) at room temperature.[25] The results of theoretical calculations (B3LYP/6-31G(d)) on radical cation **18**$^{\bullet+}$ indicated that the spin is mostly localized on the 2,5-positions and this spin is conveyed to the corresponding four equivalent *anti*-protons of the ethano bridge with an a_H value of 0.323 mT in good agreement with the observed value.

Reflecting the high spin density on 2,5-positions, radical cation **18**$^{\bullet+}$ reacted with triplet oxygen smoothly in CH_2Cl_2 to give a pale yellow SbF_6^- salt of cation **20**$^+$, which is remarkably stable, in 55% yield (Scheme 8). The structure of **20**$^+SbF_6^-$ was determined by X-ray crystallography to have an unusual proton-chelating 2-butene-1,4-dione system, as shown in Fig. 5.[25] Among the ^{1}H NMR data of the cation

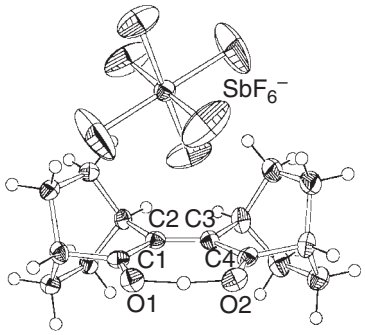

Fig. 5. ORTEP view of $\mathbf{20}^{+}SbF_6^{-}$ (50% probability). Selected bond length (Å): O1–C1 1.242(3), C1–C2 1.489(4), C2–C3 1.355(4), C3–C4 1.480(4), C4–O2 1.252(3).

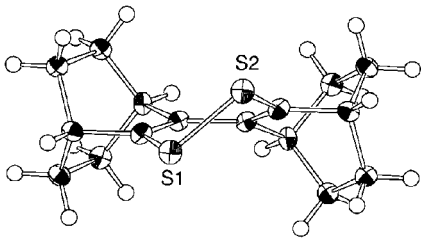

Fig. 6. ORTEP drawing of **19** (50% probability).

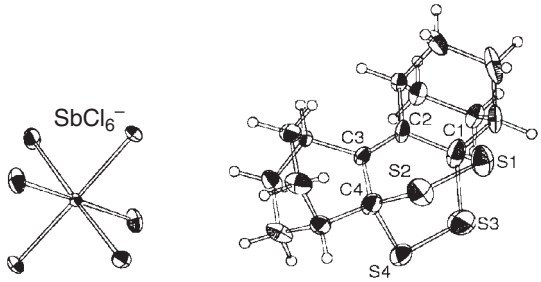

Fig. 7. ORTEP drawing of $\mathbf{21}^{\bullet+}SbCl_6^{-}$ (50% probability).

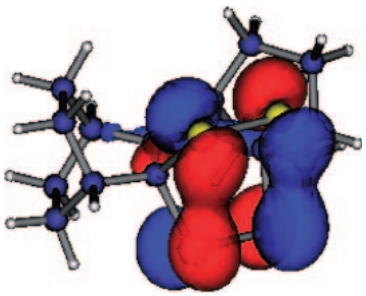

Fig. 8. The MO interaction diagram of HOMO of $\mathbf{21}^{\bullet+}$ calculated at UB3LYP/6-31G(d) level.

$\mathbf{20}^{+}$, it is noteworthy that the signal of the chelated proton was observed at such a low field (21.15 ppm). This indicates that the proton not only carries an almost full positive charge but is also subjected to the strong deshielding effect of the two carbonyl groups.

1.5.2 1,2-Dithiin Annelated with Bicyclo[2.2.2]octene: As shown in Scheme 7b, when a toluene solution of sulfur was added instead of solid powder to the di-lithiated BCO dimer, 1,2-dithiin **19** having two BCO units was obtained as a main product in 59% yield together with thiophene **18** in 22%. 1,2-Dithiin **19** is an 8π electronic system and forms a red-colored crystal having a molecular structure with a twisted C–S–S–C bond, as shown by the ORTEP drawing in Fig. 6.[27]

In the CV, 1,2-dithiin **19** underwent stepwise one-electron oxidations at +0.18 (reversible) and +0.81 (irreversible) V vs. Fc/Fc^{+}. Chemical one-electron oxidation of **19** with 1.5 equivalents of $SbCl_5$ under vacuum gave a bright yellow solution that exhibited a nine-line ESR signal. This is assigned to the radical cation $\mathbf{19}^{\bullet+}$ with ESR coupling due to the eight anti-protons with nearly equal spin densities.

Although a dilute CH_2Cl_2 solution of $\mathbf{19}^{\bullet+}$ (4×10^{-4} M) was quite stable, the radical cation was found to undergo an unexpected disproportionation when kept at a higher concentration (0.06 M). In other words, after about 5 min at room temperature, thiophene **18** (29% yield), a 2-butene-1,4-dione derivative formed by deprotonation of cation $\mathbf{20}^{+}$ (23%), and orange-colored crystals identified as the $SbCl_6^{-}$ salt of a radical cation (32%), which has a novel 2,3,5,6-tetrathiabicyclo[2.2.2]oct-7-ene structure $\mathbf{21}^{\bullet+}$ by X-ray crystallography (Fig. 7), were obtained.[27] This salt was remarkably stable and showed no decomposition upon standing in air for at least one week.

In radical cation $\mathbf{21}^{\bullet+}$, the two disulfide linkages are fixed in such close proximity as S1···S3 and S2···S4 of 2.794(3) Å. This is longer than the typical S–S bond length (2.0 Å) in alkyl disulfide but much shorter than the sum of van der Waals radii of a sulfur atom (3.70 Å), suggesting the presence of a strong transannular interaction between these sulfur atoms. The optimized structure of $\mathbf{21}^{\bullet+}$ calculated at the UB3LYP/6-31G* level reproduced the observed structure fairly well with the calculated S1···S3 and S2···S4 distances being 2.923 Å. The calculation also indicated that spin and charge of radical cation $\mathbf{21}^{\bullet+}$ are almost exclusively localized on sulfur atoms: the spin and Mulliken charge on each of the four sulfur atoms are 0.229 and +0.258, respectively. In general, the sulfur radical cation tends to form a two-center three-electron (2c–3e) S–S bond with a sulfur atom of another molecule. This can take place intramolecularly, and thus, the electronic structure of $\mathbf{21}^{\bullet+}$ can be described as a 4c–7e system. In fact, based on the B3LYP calculations, a strong interaction between the p-type sulfur lone pair orbitals can be seen in the HOMO (Fig. 8).[27]

The reaction pathway involving the disproportionation of radical cation $\mathbf{19}^{\bullet+}$ is shown in Scheme 9, which should afford products derived from thiophene radical cation $\mathbf{18}^{\bullet+}$ and radical cation $\mathbf{21}^{\bullet+}$ in a 2:1 ratio. This is close to the observed experimental result.

1.5.3 1,4-Dithiin Annelated with Bicyclo[2.2.2]octene: 1,4-Dithiin has a boat-shaped structure with 8π-electrons,[28] which is also isoelectronic to cyclooctatetraene. 1,4-Dithiin **22** annelated with two BCO units was synthesized by treating bis(3-oxobicyclo[2.2.2]oct-2-yl) sulfide with Lawesson's reagent,[29] as shown in Scheme 10.

In the CV, reversible stepwise oxidation waves were observed at such low potentials as 0.00 and 0.82 V vs. Fc/Fc^{+}. Chemical oxidation of **22** with SbF_5 in CH_2Cl_2 gave radical cation salt $\mathbf{22}^{\bullet+}SbF_6^{-}$ in 67% yield as brown-colored single

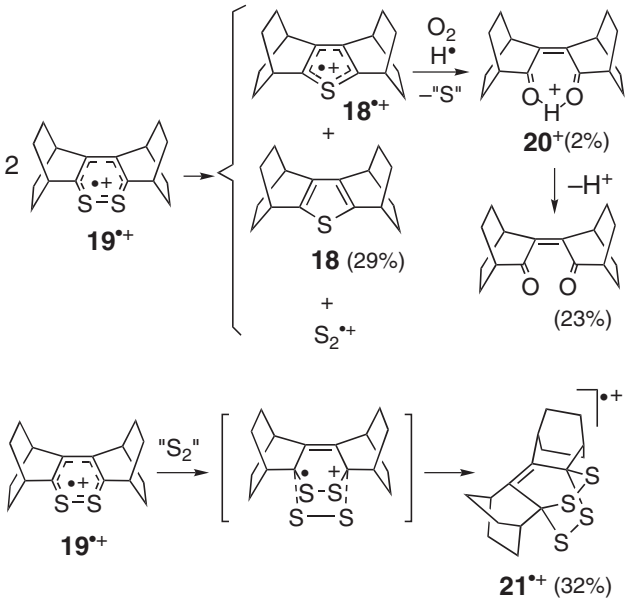

Scheme 9.

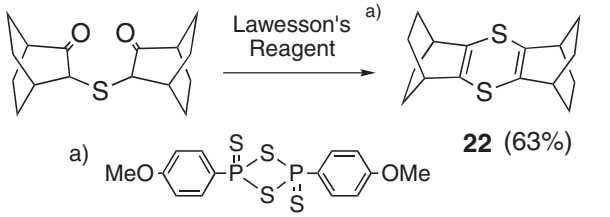

Scheme 10.

crystal, which was quite stable under air for several days. The X-ray crystallography on this salt indicated that the dithiin ring is planar with marked shortening of the C–S bond as compared with that of neutral **22** as shown in Fig. 9.[30]

A dilute CH_2Cl_2 solution of $\mathbf{22}^{\bullet+}SbF_6^-$ ($\approx 10^{-5}$ M) showed a nine-line ESR signal due to eight equivalent *anti*-protons ($a_H = 0.08$ mT, $g = 2.0083$). In the spectrum of a solution with a higher concentration ($\approx 10^{-3}$ M), the hyperfine splitting was lost, but the signal caused by $M_S = \pm 3/2$ of ^{33}S (natural isotopic abundance, 0.75%) became observable. The obtained value of a_S was 0.86 mT,[30] which is smaller than that (0.92 mT) for thianthrene radical cation ($\mathbf{23}^{\bullet+}$) (Chart 4).[31] This result indicates that the spin density on the sulfur atom of $\mathbf{22}^{\bullet+}$ is lower than that of $\mathbf{23}^{\bullet+}$, and therefore, the BCO units are even more effective in delocalizing both the positive charge and spin density than the fused benzene rings.

1.5.4 Oligothiophenes Annelated with Bicyclo[2.2.2]-octene: Oligothiophenes are subjects of growing current interest in the field of applied chemistry. They have more ordered molecular and crystalline structures than the corresponding polymers.[32] Studies on oligothiophenes are also important for elucidation of the conduction mechanism of polythiophenes and related polymers. Particularly, the radical cation and dication of oligothiophenes are considered to be important models of partial structures of p-doped polythiophene, i.e., polaron and bipolaron.[33] Based on the results described in

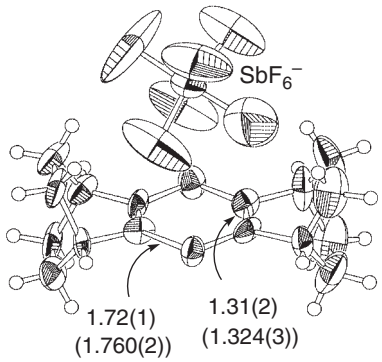

Fig. 9. ORTEP drawing of the X-ray structure of $\mathbf{22}^{\bullet+}SbF_6^-$. Bond lengths are shown in Å together with those for neutral **22** in parentheses.

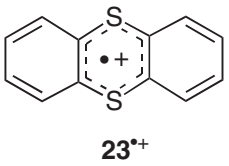

23•+

Chart 4.

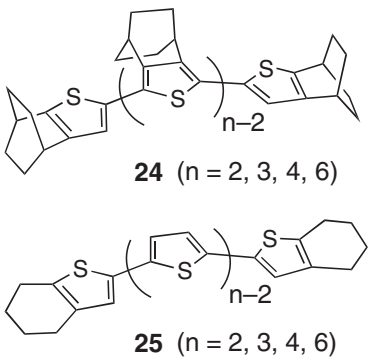

Chart 5.

the foregoing sections, it was expected that the oligothiophenes entirely surrounded by BCO frameworks should be good candidates for the positively charged species of this type of molecules with unusual stability. Furthermore, the problem of π-dimer formation[34] observed in most of oligothiophene radical cations is expected to be prevented by the steric effect of the σ-frameworks. Thus, a series of oligothiophenes **24** ($n = 2$, 3, 4, and 6) were synthesized utilizing Stille cross coupling and oxidative coupling at the 2-position of the thiophene derivatives (Chart 5).[35]

In the CV of **24** ($n = 2$, 3, 4, and 6), two-step oxidation waves, which are all completely reversible and at lower potentials than the oligothiophenes end-capped with cyclohexene **25**[36] (Table 2), were observed, suggesting the formation of stable radical cations and dications.

In accord with this, chemical one-electron oxidation of dimer and trimer **24** ($n = 2$ and 3) with one equivalent of $NO^+SbF_6^-$ in CH_2Cl_2 under vacuum took place smoothly and afforded stable single crystals of radical cation salts $\mathbf{24}^{\bullet+}SbF_6^-$ ($n = 2$, deep green, 61%; $n = 3$, deep purple,

Table 2. Oxidation Potential ($E_{1/2}$, V vs. Fc/Fc^+)[a] of **24** and **25**

	24		**25**[b]	
n	$E_{1/2}$ (1)	$E_{1/2}$ (2)	$E_{1/2}$ (1)	$E_{1/2}$ (2)
2[c]	+0.47	+1.07	(+0.53)[d]	(+1.20)[d]
3	+0.27	+0.70	+0.38	(+0.79)
4	+0.19	+0.46	+0.32	+0.66
6[c]	+0.19	+0.28	+0.22	+0.41

a) Determined by cyclic voltammetry in CH_2Cl_2 containing 0.1 M Bu_4NPF_6 at 25 °C; scan rate 100 mV s^{-1}. b) Ref. 36. c) At −78 °C. d) Irreversible peak potential.

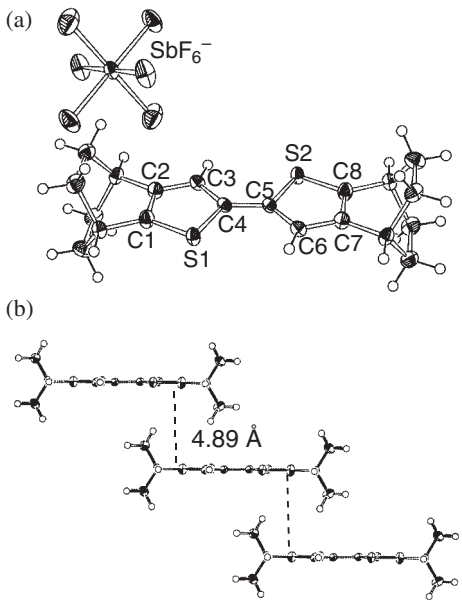

Fig. 10. (a) X-ray structure of radical cation salt $\mathbf{24}^{\bullet+}$-SbF_6^- ($n = 2$). Selected bond lengths (Å) and angles (deg) are: S1–C1, 1.696(5); C1–C2, 1.408(6); C2–C3, 1.371(6); C3–C4, 1.403(6); C4–S1, 1.752(4); C4–C5, 1.398(8); C3–C4–C5–C6, 180.0. (b) Crystal packing drawing; the SbF_6^- ions are omitted for clarity.

73%).[37] These crystals did not show any decomposition even after being left at room temperature in air for one month. This was the first time that X-ray crystallography was conducted on a radical cation salt of bithiophene ($\mathbf{24}^{\bullet+}$; $n = 2$), and it showed that the π-system is completely planarized, as shown in Fig. 10. This planarization is accompanied by considerable shortening of the inter-ring bond (1.398(8) Å) as compared with that in neutral **24** ($n = 2$) (1.455(3) Å), showing that the double bond character of this bond is greater and the quinoidal structure shown in Scheme 11 has the greatest contribution. Similarly, the molecular structure was determined for $\mathbf{24}^{\bullet+}$-SbF_6^- ($n = 3$), which has inter-ring bonds that are a little more twisted (Fig. 11).[37]

In contrast to these two cases, the treatment of oligothiophene tetramer and hexamer **24** ($n = 4$ and 6) with one equivalent of $NO^+SbF_6^-$ afforded not the radical cation but the dication salts $\mathbf{24}^{2+}2SbF_6^-$ ($n = 4$ and 6) as dark green crystals with gold luster in 26% and 46% yield, respectively. The yield increased to 46% and 73%, respectively, when two equivalents

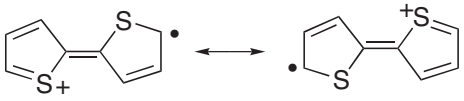

Scheme 11.

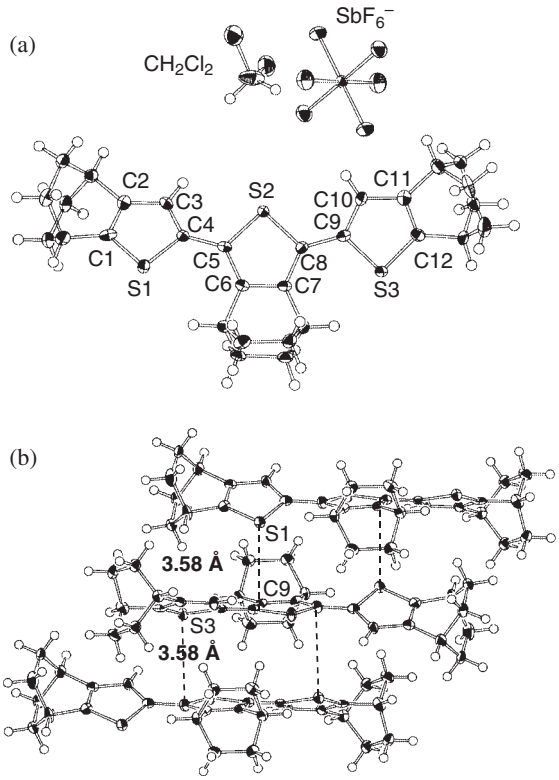

Fig. 11. (a) X-ray structure of radical cation salt $\mathbf{24}^{\bullet+}$-SbF_6^- ($n = 3$). Selected bond lengths (Å) and angles (deg) are: S1–C1, 1.697(6); C1–C2, 1.394(9); C2–C3, 1.389(11); C3–C4, 1.390(11); C4–S1, 1.761(6); C4–C5, 1.421(9); C5–C6, 1.424(9); C6–C7, 1.389(9); C7–C8, 1.418(9); C8–S2, 1.747(6); S2–C5, 1.751(6); C8–C9, 1.436(9); C9–S3, 1.755(6); C9–C10, 1.389(12); C10–C11, 1.411(11); C11–C12, 1.372(10); C12–S3, 1.706(6); C3–C4–C5–C6, −155.5(8); C7–C8–C9–C10, −149.4(8). (b) Crystal packing drawing; the SbF_6^- ions and CH_2Cl_2 are omitted for clarity.

of the oxidant were used. X-ray crystallography was conducted for the first time on dications of oligothiophenes $\mathbf{24}^{2+}2SbF_6^-$ ($n = 4$ and 6).[37] Again, the π-system of the terthiophene dication $\mathbf{24}^{2+}2SbF_6^-$ ($n = 4$) was found to be completely planar with all the thiophene rings in *anti* conformation (Fig. 12) but the planarity was slightly less in the sexithiophene dication $\mathbf{24}^{2+}2SbF_6^-$ ($n = 6$) as shown in Fig. 13. From a comparison of the C–C bond lengths in the π-conjugated system, C(α)–C(β) bonds in the terminal thiophene rings were found to be shorter than the C(β)–C(β') bonds, whereas they become longer than the C(β)–C(β') bonds in the rings closer to the center in both dications $\mathbf{24}^{2+}2SbF_6^-$ ($n = 4$ and 6). This indicates that the electronic structure of the terminal rings is closer to that of neutral thiophene, whereas the quinoidal character becomes greater in the rings closer to the central position.[37]

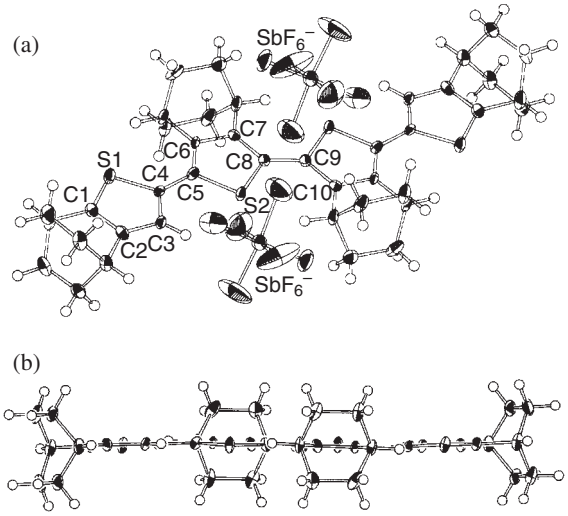

Fig. 12. (a) X-ray structure of dication salt $\mathbf{24}^{2+}(SbF_6^-)_2$ ($n = 4$). Selected bond lengths (Å) and angles (deg) are: S1–C1, 1.668(6); C1–C2, 1.372(8); C2–C3, 1.385(8); C3–C4, 1.388(8); C4–S1, 1.743(6); C4–C5, 1.383(7); C5–C6, 1.408(8); C6–C7, 1.358(7); C7–C8, 1.417(8); C8–S2, 1.733(6); S2–C5, 1.730(6); C8–C9, 1.390(11); C3–C4–C5–C6, −179.6(6); C7–C8–C9–C10, 180.0. (b) Side view with the counter anions SbF_6^- are omitted for clarity.

1.5.5 Terthiophene End-Capped with Bicyclo[2.2.2]-octene: In all of the cases described in the previous section, annelation with the BCO units all around the molecules of oligothiophene radical-cation was shown to be effective in prevention of the formation of π-dimers so that the elucidation of geometrical and electronic structure of these radical cations as single molecules became possible. Then, we became interested in investigating the radical cation of an oligomer, such as terthiophene, which has the steric protection with the BCO units only at the both ends of the molecule.

Thus, terthiophene end-capped with BCO units **26** (Chart 6) was synthesized by palladium-catalyzed cross coupling of 2,5-dibromothiophene with 2-stannylthiophene annelated with a BCO unit.[38] In the CV of **26**, there was a reversible oxidation wave at $E_{1/2}$ +0.31 V vs. Fc/Fc^+, which is 0.04 V higher than that of **24** ($n = 3$) due to the loss of an electron-donating BCO unit. Upon one-electron oxidation with $NO^+SbF_6^-$, terthiophene **26** was converted to deeply blue-colored radical-cation salt $\mathbf{26}^{\bullet+}SbF_6^-$, which is highly stable under air, in 88% yield. The UV–vis–NIR spectrum of a solution of radical cation $\mathbf{26}^{\bullet+}$ in CH_2Cl_2 exhibited a temperature dependency, in which the spectra of the monomeric species decreased with a concomitant increase in that for the corresponding π-dimer as the temperature was lowered to 180 K. The same disappearance of the monomeric species was also observed by using ESR spectroscopy.[38]

More clear-cut evidence for the π-dimer formation was obtained from the X-ray crystallography on the single crystal of $\mathbf{26}^{\bullet+}SbF_6^-$. As shown in Fig. 14a, units of radical cation $\mathbf{26}^{\bullet+}$ are paired, and each cationic unit in a pair strongly interacts with each other, as indicated by mutual attraction at the central part where the steric hindrance is minimal. Accordingly, the molecules are considerably bent. The closest intermolecular

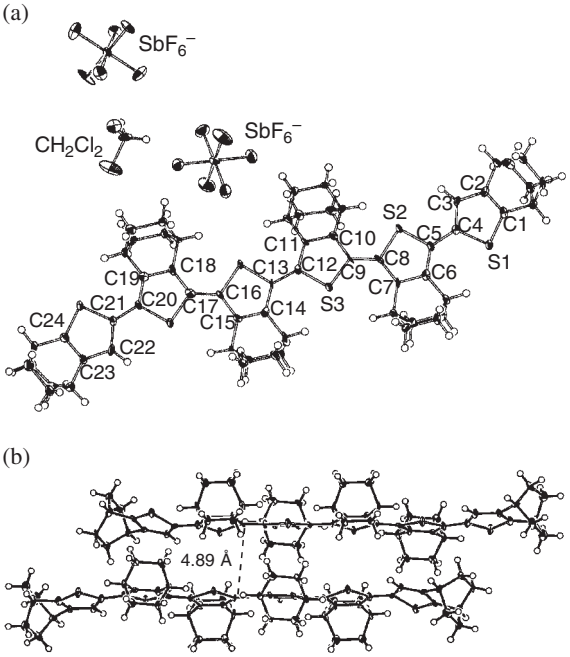

Fig. 13. (a) X-ray structure of dication salt $\mathbf{24}^{2+}(SbF_6^-)_2$ ($n = 6$). Selected bond lengths (Å) and angles (deg) are: S1–C1, 1.717(11); C1–C2, 1.370(14); C2–C3, 1.419(14); C3–C4, 1.393(14); C4–S1, 1.775(10); C4–C5, 1.442(14); C5–C6, 1.411(14); C6–C7, 1.404(13); C7–C8, 1.417(14); C8–S2, 1.767(10); S2–C5, 1.747(10); C8–C9, 1.418(14); C9–C10, 1.439(14); C10–C11, 1.402(14); C11–C12, 1.438(14); C9–S3, 1.740(10); S3–C12, 1.769(10); C12–C13, 1.410(13); C3–C4–C5–C6, 178.0(11); C7–C8–C9–C10, 158.8(11); C11–C12–C13–C14, 161.6(11); C15–C16–C17–C18, −173.2(11); C19–C20–C21–C22, 169.9(11). (b) Side view with counter anions SbF_6^- are omitted for clarity.

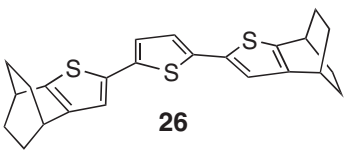

26

Chart 6.

distances are 2.976(10) Å between the two C_β atoms of the central rings and 3.091(10) Å between the C_α atoms. It is remarkable that such a strong attractive interaction operates between the two positively charged species. This clearly indicates that a π–π interaction can overcome the electrostatic repulsion and destabilization by structural deformation. This strong interaction was confirmed by a single point energy calculation for the KS HOMO of the π-dimer at the B3LYP/6-31+G(d) level. As shown in Fig. 14b, there is substantial overlap of the SOMOs of $\mathbf{26}^{\bullet+}$ in the center.[38]

In solid state at 300 K, the ESR spectrum of $\mathbf{26}^{\bullet+}SbF_6^-$ exhibited only a single-line signal presumably due to the monomeric radical cation present as a contaminant. However, as shown in Fig. 15, when the sample was heated to 400 K a new triplet-state signal was observed ($D = 127$ G, $E = 23$ G), which was assigned to a thermally excited triplet state of the

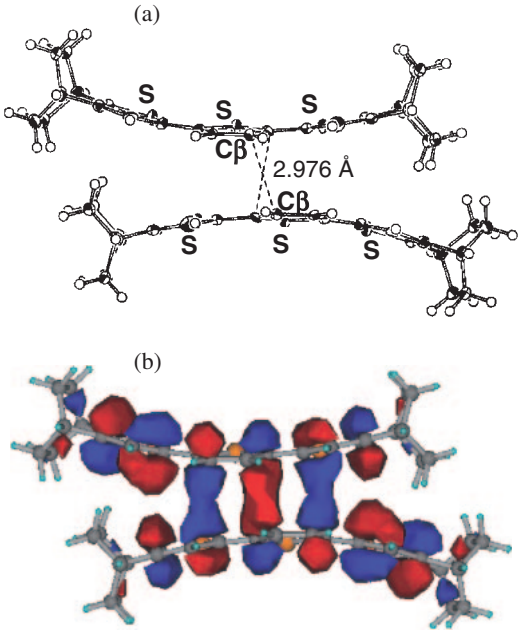

Fig. 14. (a) ORTEP drawing of the π-dimer moiety $(\mathbf{26}^{\bullet+})_2$. (b) Calculated KS-HOMO using the structure determined by X-ray structural analysis.

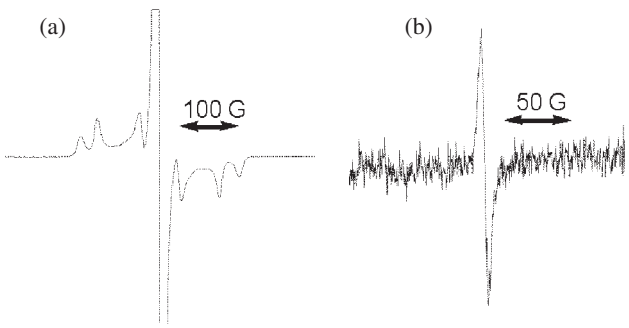

Fig. 15. a) An ESR spectrum of $\mathbf{26}^{\bullet+}$ exhibiting a signal for thermally accessible triplet state of π-dimer $(\mathbf{26}^{\bullet+})_2$ and that for monomeric $\mathbf{26}^{\bullet+}$ ($g = 2.0016$). b) A signal at a half-field ($g = 4.0072$).

π-dimer. At a half-field ($g = 4.0072$), a weak signal emerged at 400 K and disappeared at 300 K, in accord with the above observation. This can be taken as the first observation of the triplet state of the radical-cation π-dimer that was thermally generated.[38]

1.6 Cyclic π-Conjugated Systems Annelated with Bicyclo[2.1.1]hexene. As compared with bicyclo[2.2.2]octene (BCO), a σ-bond in a smaller bicyclic system, e.g., bicyclo[2.1.1]hexene (abbreviated as BCH), has a stronger p-character, and should be more advantageous in σ–π conjugation. However, because of its inherent strain, annelation with BCH inevitably impose considerable ring strain upon the annelated π-system as well as double-bond fixation. Thus, annelation with BCH is considered to be less advantageous in stabilization of cationic π-systems.[39]

On the other hand, Siegel and co-workers have prepared a benzene tris-annelated with BCH units, **27**,[40] and have found that the bond-fixation effect is so great that the benzene ring

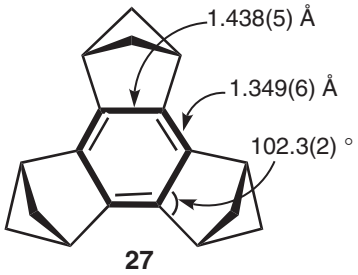

Fig. 16. Bond-alternated benzene **27** with the bond lengths determined by X-ray crystallography.[41]

assumes the structure of cyclohexatriene (Fig. 16).[41] Thus, the properties, such as aromaticity and reactivity, of **27** are quite intriguing, but these have not been scrutinized because of extremely low yield in the synthesis of **27** (<1%).[40] Therefore, we decided to synthesize benzene **27** more efficiently.

1.6.1 Benzene Tris-Annelated with Bicyclo[2.1.1]hexene: We utilized the intermolecular cross-coupling reaction of lithium cuprate generated from 2,3-diiodobicyclo[2.1.1]hexene **28**, which was synthesized from bicyclo[2.1.1]hexan-2-one[42] as shown in Scheme 12. This method successfully allowed us to obtain not only the cyclotrimer, i.e., benzene **27**, but also the cyclotetramer, i.e., cyclooctatetraene (COT) **29**, in 43% and 21% yields respectively.[43]

As shown in Table 3, benzene **27** retains a certain extent of aromaticity as demonstrated by three different criteria: nucleus independent chemical shift (NICS, ppm), aromatic stabilization energy (ASE, kcal mol^{-1}), and magnetic susceptibility exaltation (Λ, ppm). Interestingly, however, **27** smoothly underwent all-cis tris-epoxidation with *m*-chloroperbenzoic acid and all-cis tris-cyclopropanation with a modified Simmons–Smith reagent (Scheme 13) as if it were cyclohexatriene.[43]

The HOMO level of benzene **27** is considered to be elevated because of a strong σ–π interaction with the BCH units. Thus, one-electron oxidation of **27** with 1.5 equiv of $SbCl_5$ in CH_2Cl_2 readily proceeded at 0 °C to give novel naphthalene **30** in 29% yield.[44] A possible mechanism for this transformation involves formation of the unstable radical cation $\mathbf{27}^{\bullet+}$ and aromatization of one of the BCH units as shown in Scheme 14.

The molecular structure of **30** was determined by X-ray crystallography at 100 K (Fig. 17). Corresponding bond lengths of parent naphthalene[45] are also shown for comparison. As expected from the BCH annelation, C1–C2 and C3–C4 bonds are longer and C1–C8a and C2–C3 bonds are shorter. As a result, the extent of bond alternation in the BCH-annelated six-membered ring becomes much smaller than that in the mother compound and that in the non-annelated six-membered ring.

The degree of aromaticity of the two six-membered rings in naphthalene **30** was examined by using two different indexes. The Harmonic Oscillator Model of Aromaticity (HOMA),[46] which is a geometry-based aromaticity index, was calculated based on the X-ray crystal structure. The value for the BCH-annelated ring of **30** was 0.843, which is larger and closer to the value for benzene (0.979)[46b] than that of parent naphthalene (0.789). In contrast, that (0.582) of the non-annelated ring is considerably smaller. The NICS,[47] an aromaticity index based on magnetic property, also showed the same tendency: the value for BCH-annelated ring of **2** was calculated as

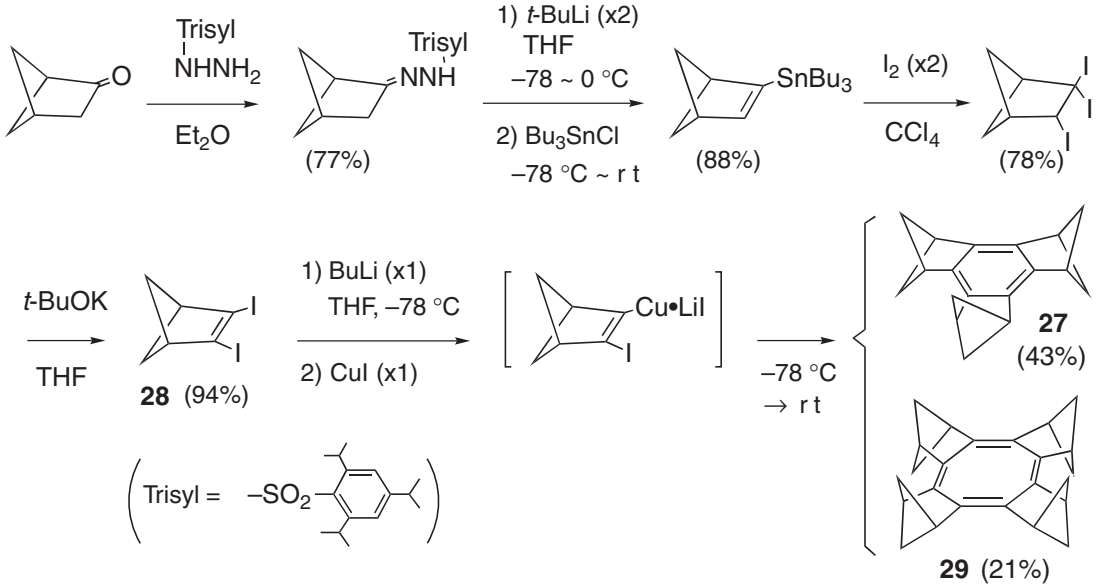

Scheme 12.

Table 3. Aromaticity/Antiaromaticity Criteria for Ordinary Benzene, Benzene **27**, Hypothetical Planar COT, and COT **29**

Compd	ASE[a)]	Λ[b)]	NICS[c)]
Benzene	−34.1	−16.2	−9.7
27	−34.0	−8.4	−8.0
Planar COT	2.9	61.1	27.2
29	4.1	17.2	10.6

a) Aromatic stabilization energy in kcal mol^{-1} (B3LYP/6-311+G**). b) Magnetic susceptibility exaltation in ppm (CSGT-HF/6-31G+G**). c) Nucleus independent chemical shift in ppm (GIAO-HF/6-31+G**).

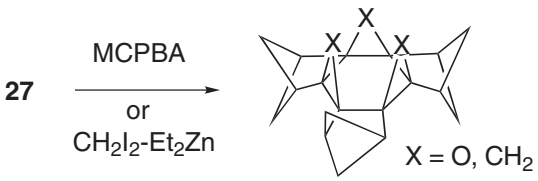

Scheme 13.

−11.8, which is even more negative (i.e., more aromatic) than that of parent naphthalene (−9.9), whereas that for the non-annelated ring was calculated as −7.5. Thus, **30** represents a unique naphthalene, in which one six-membered ring is aromatic and the other is olefinic.[44]

1.6.2 Cyclooctatetraene (COT) Tetra-Annelated with Bicyclo[2.1.1]hexene: It was anticipated that the COT annelated with bicyclo[2.1.1]hexene (BCH) **29** would take a planar conformation, because double bonds should be positioned out of the BCH units in order to minimize the steric strain.[48] In fact, the molecular structure of **29**, determined by X-ray crystallography, shows that the central eight-membered ring is entirely planar (Fig. 18). The bond lengths are alternatively shorter (average 1.331(1) Å) and longer (average 1.500(1) Å) with the shorter bonds exocyclic to bicycloannelation. As to

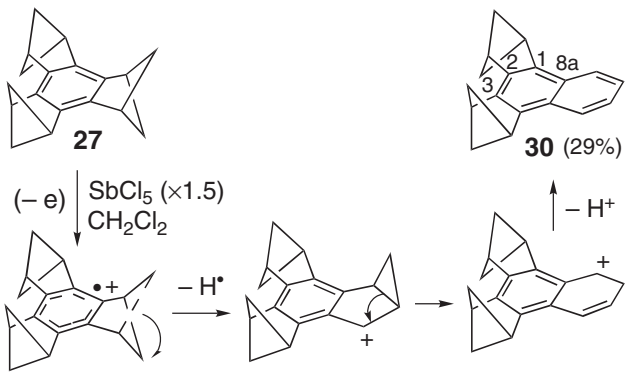

Scheme 14.

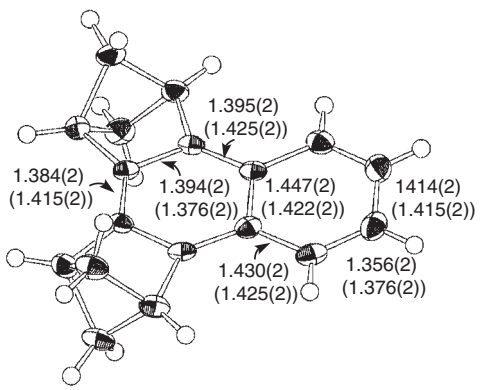

Fig. 17. ORTEP drawing and bond lengths (Å) of naphthalene **30** together with those for parent naphthalene shown in parentheses (Ref. 44).

the COT having planar geometry, only a few examples, such as **31** having perfluorocyclobutene rings,[49] and benzoderivatives as exemplified by **32**[50] and **33**,[51] are known (Chart 7). Thus, compound **29** is the first non-benzoannelated hydrocarbon with a completely planar COT ring.

As has been shown in Table 3, although the destabilization

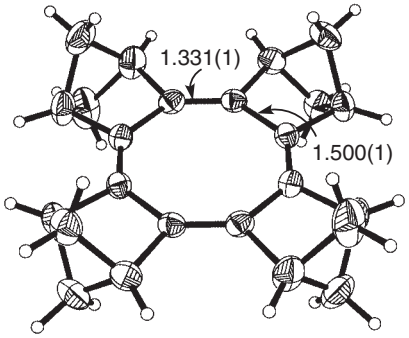

Fig. 18. ORTEP drawing and bond lengths (Å) of COT **29**.

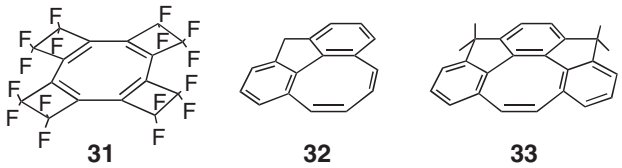

Chart 7.

energy of **29** slightly exceeds that of the hypothetical D_{4h} planar COT, the NICS value (10.6) as well as the Λ value (17.2) is considerably less than those of the D_{4h} planar COT. Such reduction of antiaromaticity of **29** might be attributed to an enhanced bond alternation ($\Delta R = 0.161$ Å) relative to that in the D_{4h} planar COT ($\Delta R = 0.132$ Å). However, the NICS value of the hypothetical molecule, tetrakis(cyclobuteno)COT, which has the same degree of bond alternation ($\Delta R = 1.491$ Å $- 1.336$ Å $= 0.155$ Å) as **29**, reveals considerable retention of antiaromaticity (NICS: 20.9). Thus, the σ–π interaction between 1,3-bridged cyclobutane subunits in the bicyclohexene frameworks and the planar COT ring must be responsible for the change in the inherent magnetic properties and the reduced antiaromaticity of the present 8π electronic system **29**.

The UV–vis spectrum of **29** in CH_2Cl_2 exhibited the longest wavelength absorption at 459 nm (ε 130).[43] This value is red-shifted by 177 nm compared with that of tetrakis(bicyclo[2.2.2]octeno)COT (**34**)[52] ($\lambda_{max} = 282$ nm, ε 800) with the tub-shaped COT ring, indicating that planarization of the COT ring in **29** causes a substantial decrease in the HOMO–LUMO gap (Chart 8).

The influence of the σ–π interaction and planarization on the electronic structure of COT was also demonstrated by the oxidation potential of **29** as measured by using cyclic voltammetry in CH_2Cl_2. COT **29** exhibited a well-defined reversible oxidation wave at +0.07 V vs. Fc/Fc^+ and an irreversible one at +0.76 V. These potentials are lower by ca. 0.4 V than corresponding values for **34**, which is evidently due to a raise of the HOMO of the eight-membered ring.

Reflecting such a higher level of HOMO, COT **29** was readily oxidized with $SbCl_5$ in CS_2 to give dark purple crystals of the radical cation salt $\mathbf{29}^{\bullet+}SbCl_6^-$. Although the crystal was not large enough for X-ray crystallography, the ESR spectrum of the CH_2Cl_2 solution exhibited a spectrum that could be simulated by using the calculated structure with a planar eight-membered ring (Fig. 19).[53]

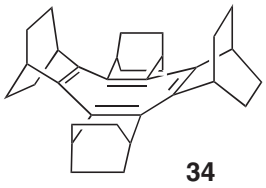

Chart 8.

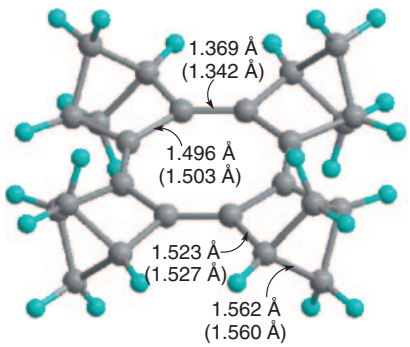

Fig. 19. Optimized structure of $\mathbf{29}^{\bullet+}$ at the B3LYP/6-31G* level. Calculated C–C bond lengths and the corresponding lengths of neutral **29** in parentheses are shown.

1.7 Concluding Remarks. The present study clearly demonstrated that full annelation of various cyclic π-conjugated systems with bicyclic σ-frameworks has remarkable effects of elevation of the π-systems' HOMO level and stabilization of the corresponding cationic systems. The poly-annelation with bicyclo[2.2.2]octene frameworks can generate various cationic species, which could not be prepared by any other means, and even allowed characterization by X-ray crystallography in many cases. These include radical cation salts of a series of polycyclic aromatic hydrocarbons and sulfur-containing systems such as thiophene, 1,2- and 1,4-dithiins, and oligothiophenes. The closed-shell tropylium ion with extraordinary stability was prepared, and the first example of silatropylium ion was generated in solution. The bicyclic frameworks can also be utilized for ^{13}C NMR observation of the site exchange of coordination of alkali metal ion to a Cp anion, and annelation with a polycyclic unit such as homoadamantene was found to stabilize the bond localized Cp radical.

On the other hand, poly-annelation with more strained bicyclo[2.1.1]hexene (BCH) frameworks was shown to bring about notable bond alternation and unusual electronic states to the π-systems. Thus, a naphthalene with an unusual electronic state was synthesized from a benzene derivative. A COT tetra-annelated with the BCH units was shown to have planar geometry with considerably lowered antiaromaticity.

So far, p–π or n–π conjugation has been utilized as a means to control the electronic structure of π-systems. Results of the present study indicate that σ–π interaction (C–C hyperconjugation), which has been considered as a relatively weak interaction, can exert significant effects upon the properties of the π-systems when the maximal number of σ-bonds are fixed in a nearly parallel position to 2p orbitals. This might become useful in design of a new stable cationic species, which can play an important role in applications.

2. A Molecular Surgical Approach to Endohedral Fullerenes

Fullerenes are spherical carbon clusters that have empty inner space. Since the representative member of fullerenes, C_{60}, was first isolated in 1990,[8b] an enormous number of studies have been reported concerning the exterior structural modification of fullerenes.[9] In contrast, the study on the interior of fullerenes has been much limited mostly due to the difficulty in obtaining a sufficient amount of endohedral fullerenes, i.e., the fullerenes encapsulating atom(s) or a molecule in their empty cavity, in spite of great interest in these particular class of fullerenes both from fundamental significance and from application-oriented study.[54] This problem originates from the fact that the production of endohedral fullerenes has only relied on rather classical physical methods, such as arc-discharge of metal oxide–graphite composite rods or high-pressure/high-temperature treatment of the fullerenes under noble gases.[55] The species that have been encapsulated are largely metals and noble gas atoms, but, again, the availability of these endohedral fullerenes is only a few milligrams after laborious separation procedures. On the other hand, Rubin et al. have proposed a molecular surgical approach to endohedral fullerenes, which involves opening a hole on fullerene's cage and encapsulating a small guest species.[56,57] In fact, he has synthesized a derivative of the fullerene with an orifice that is a 14-membered ring **35** (Chart 9) and has succeeded in encapsulating molecular hydrogen and helium in 5% and 1.5% respectively.[56] In Section **2** of this article, the author will describe his own research conducted independently from Rubin's work to encapsulate hydrogen in 100% in an open-cage fullerene and to complete restoration of the cage to furnish an endohedral fullerene encapsulating molecular hydrogen, i.e., $H_2@C_{60}$.

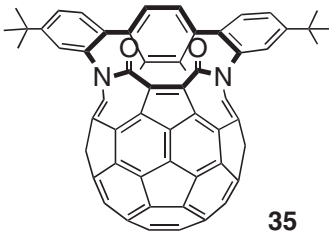

35

Chart 9.

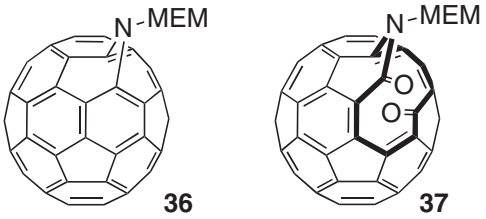

36 **37**

Chart 10.

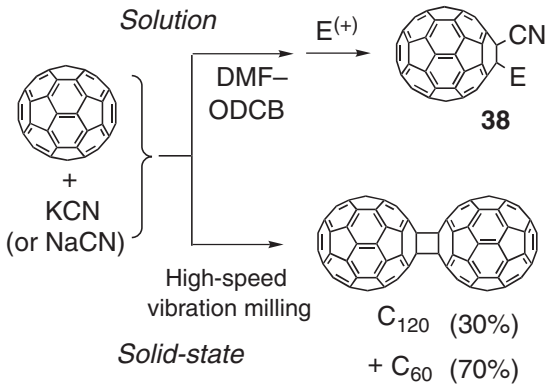

Scheme 15.

2.1 Solid-State Reaction vs. Liquid-Phase Thermal Reaction. In 1995, Wudl and co-workers have reported the synthesis of a first open-cage fullerene, i.e., ketolactam **37** (Chart 10) having an 11-membered-ring orifice, through the reaction of [5,6]-azafulleroid **36** with singlet oxygen.[58] However, the orifice was found to be too small even for a helium atom to pass through at temperatures as high as 200 °C.[57]

We, on the other hand, were interested in the solid-state reaction of fullerene C_{60}. It was found that some reactions take entirely different courses depending on the reaction phase. For example, the reaction of C_{60} with NaCN gives cyanated C_{60} derivative **38** in a liquid-phase reaction[59] but it selectively affords a dumbbell-shaped fullerene dimer, C_{120}, under the solid-state mechanochemical reaction conditions (Scheme 15).[60]

This study was further extended to the reaction of C_{60} with polyaza-aromatic compounds.[61] As a typical example, the solid-state reaction of C_{60} with phthalazine (2,3-diazanaphthalene) was found to give a dimer of C_{60} with the two C_{60} cages incorporated in a benzobicyclo[2.2.2]octene framework **40**, whereas the same reactants when heated in solution afforded a benzo-derivative of an open-cage fullerene **41**.[62] This is rationalized as shown in Scheme 16. The common intermediate **39**, which was formed by the initial [4 + 2] reaction and nitrogen extrusion, is subjected to another dienophilic reaction by C_{60} in the case of solid-state reaction, during which no solvent is present. In contrast, intermediate **39** has to undergo the intramolecular "formal" [4 + 4] reaction, which is followed by retro [2 + 2 + 2] reaction, to produce the opening of an eight-membered-ring orifice on the C_{60} cage, when the intermediate is isolated by a solvation shell from other C_{60} molecules.[62]

2.2 The Formation of Open-Cage Fullerene and Insertion of Molecular Hydrogen. Based on the above-mentioned finding, we searched for appropriate aza-aromatics to make open-cage fullerenes and found that 5,6-diphenyl-3-(2-pyridyl)-1,2,4-triazine (**42**) is useful as will be described. When the reaction of C_{60} and **42** in *o*-dichlorobenzene (ODCB) was conducted at 180 °C for 17 h, open-cage fullerene **43** was obtained in 50% yield, or 85% yield based on consumed C_{60} (Scheme 17), according to the same mechanism as the one in Scheme 16.[63] The X-ray structure of **43** indicates that the double bonds on the rim of the orifice are considerably distorted (twist angle, 39.0 and 38.8°), and the coefficients of the HOMO are relatively high on these carbons. Thus, singlet oxygen, generated by irradiation of visible light, selectively adds to one of these double bonds, resulting in enlargement of the orifice through the formation of 1,2-dioxetane, to give **44a** and its isomer **44b** with a 12-membered-ring orifice (Scheme 18).[63]

Although the π-conjugated systems in these open-cage full-

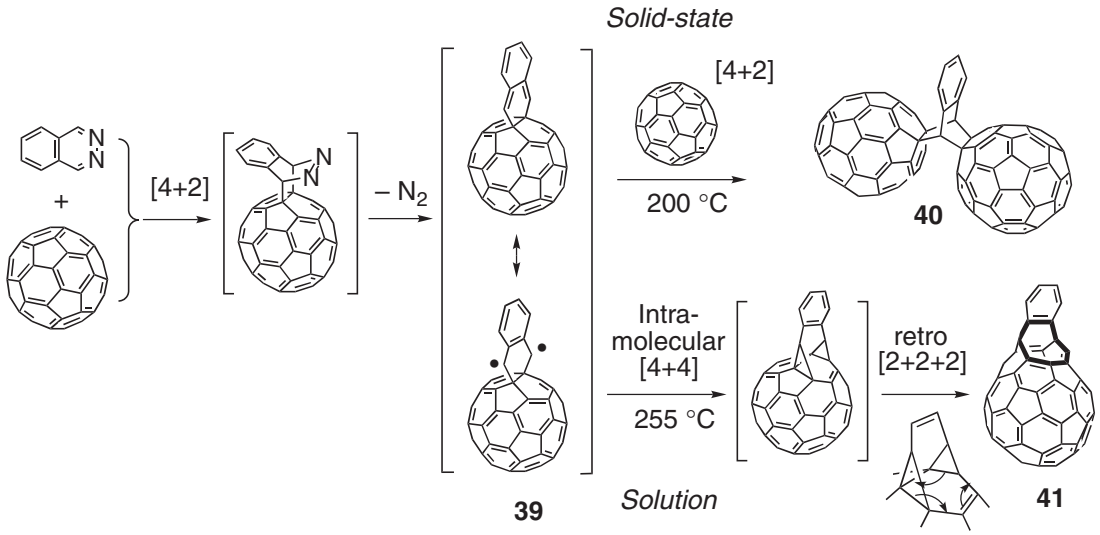

Scheme 16.

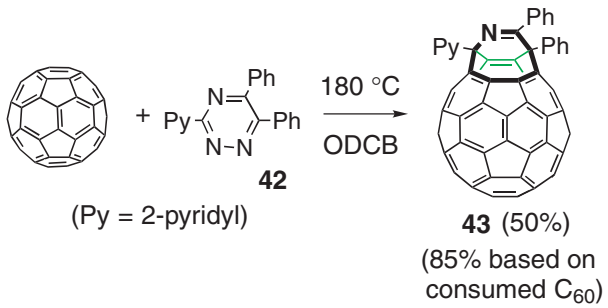

Scheme 17.

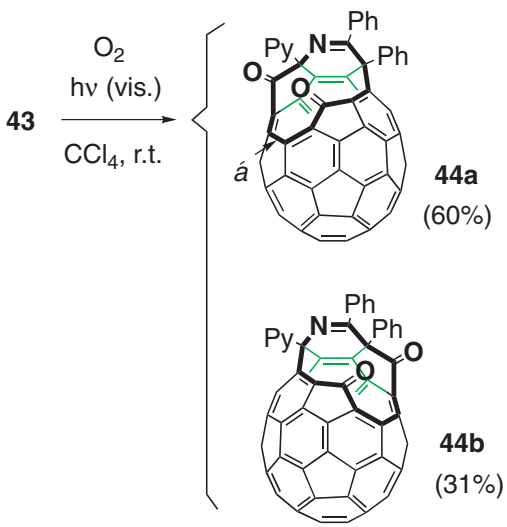

Scheme 18.

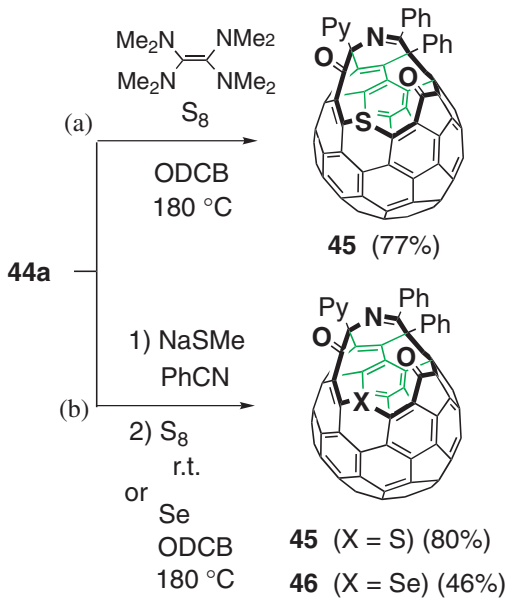

Scheme 19.

erenes (**44a** and **44b**) are severely torn out, in their cyclic voltammograms, there were four reversible reduction waves quite similar to those of C_{60} with the first and second waves at the potential even lower than C_{60} by about 0.2 V possibly due to the presence of two carbonyl groups. Thus, these open-cage fullerenes are regarded as even better electron acceptors than C_{60}. The LUMO coefficients were found to be relatively high on the butadiene unit on the rim of the orifice. It was therefore thought to be possible to insert a sulfur atom into the central part (bond a) of the butadiene unit in order to enlarge the size of the orifice if the molecule was activated by the presence of a typical π-electron donor such as tetrakis(dimethylamino)ethylene. As shown in Scheme 19a, the reaction with elemental sulfur took place by heating at 180 °C to give **45** with a 13-membered-ring orifice as a single product in 77% yield.[63]

As a more direct way for activation, open-cage fullerene **44a** can be reduced to the dianion by using 2 equivalents of sodium methylthiolate,[64] and the insertion of sulfur readily took place even at room temperature to give **45** in 80% yield (Scheme 19b).[65] In addition, this method made it possible to insert a selenium atom in place of sulfur to give **46**,[65] thus slightly enlarging the orifice, because of a slightly longer C–Se bond as compared with a C–S bond. The X-ray crystal structures of **45** and **46** are shown in Fig. 20. The lengths of the

longest axis (C7–X) and the shortest axis (C4–C10) across the opening are 5.643(3) and 3.753(3) Å for **45** (X = S) and 5.718(4) and 3.877(5) Å for **46** (X = Se).[65]

As compared to the rather elliptic shape of Rubin's open-cage fullerene **35**, the orifice of **45** is a little more circular. The required energy calculated (B3LYP/6-31G**//B3LYP/3-21G) for a hydrogen molecule to enter through the orifice of **45** is 30.1 kcal mol^{-1}, which is about 11 kcal mol^{-1} lower than that for **35** (41.4 kcal mol^{-1}). In accord with this, treatment of a powder of **45** with hydrogen gas (800 atmosphere) at 200 °C for 8 h resulted in 100% encapsulation of molecular hydrogen in **45**, thus yielding H_2@**45**.[66] The encapsulated hydrogen was detected as a singlet at such a high field as −7.25 ppm in ^{1}H NMR. The hydrogen molecule was also directly observed to be positioned at the center of the cage by synchrotron X-ray crystallography and MEM (maximum entropy method) analysis.[67]

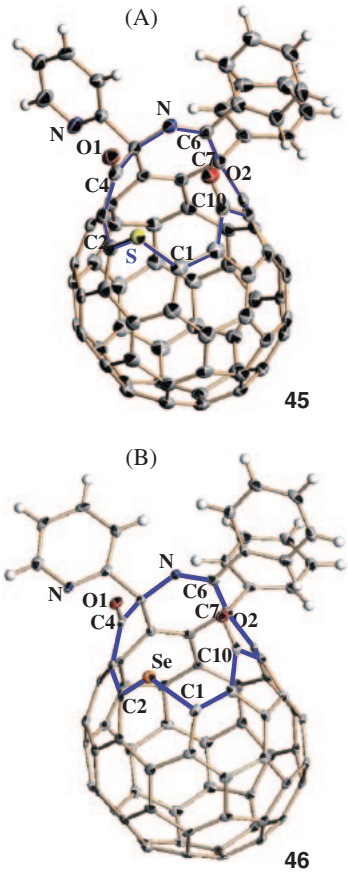

Fig. 20. X-ray crystal structures of **45** and **46**. Selected bond lengths (Å) and angles (deg): (A) **45**: C1–S, 1.754(3); C2–S, 1.780(3); C1–S–C2, 92.18(12): (B) 46: C1–Se, 1.909(4); C2–Se; 1.921(4); C1–Se–C2, 87.87(16).

H_2@**45** is quite stable at room temperature, but it released hydrogen slowly in the temperature range of 160 to 190 °C.[66] The rate followed first-order kinetics, and the activation energy was calculated to be 34.3 kcal mol^{-1}. Note that this value is close to the value calculated for a hydrogen molecule to enter through the orifice of **45** mentioned above.

2.3 Organic Synthesis of H_2@C_{60} from H_2@Open-Cage-Fullerene. In order to restore the complete shape of C_{60} cage out of open-cage fullerene, the first operation to do would be the removal of the sulfur atom out of the rim of the orifice. This was conducted by oxidation of sulfide H_2@**45** to sulfoxide H_2@**47** by treating with *m*-chloroperbenzoic acid (MCPBA) (Scheme 20a), followed by removal of the sulfinyl unit by irradiation with visible light to give H_2@**44a** (Scheme 20b). Both of these reactions were conducted at room temperature to prevent the escape of encapsulated hydrogen. Then in the next step, two carbonyl groups in H_2@**44a** were reductively coupled by treating with Ti^0 [68] at 80 °C to give H_2@**43** having an eight-membered-ring orifice as shown in Scheme 20c.[69]

At each of these three steps, complete retention of the encapsulated hydrogen was confirmed based on the integrated peak intensity (2.00 ± 0.05 H) of the characteristic upfield NMR signals of the encapsulated hydrogen (−6.18 ppm for H_2@**47**, −5.69 for H_2@**44a**, and −2.93 for H_2@**43**). The gradual downfield shift of the hydrogen signal, observed upon these transformations, reflects the formation at each step, within the fullerene cage, of a fully π-conjugated five-membered ring, which exerts a strong deshielding effect through its paramagnetic ring currents.[69b]

Finally, complete closure of the orifice was achieved by heating the powder of H_2@**43** in a glass tube under vacuum at 340 °C for 2 h (Scheme 21). The crude product dissolved in carbon disulfide was passed through a silica-gel column to give H_2@C_{60} (contaminated with 9% empty C_{60}) in 67% yield. Similar results were obtained when H_2@**43** was heated at 300 °C for 24 h, at 320 °C for 8 h, or at 400 °C for 2 min.[69]

The mechanism for this closure of the orifice (Scheme 21) is supposed to be the reversal of the one proposed for the opening of the orifice as already indicated in Scheme 17. The thermal [2 + 2 + 2] reaction near the orifice of H_2@**43** gives the bis-(cyclopropane) intermediate H_2@**48**, which then cleaves to

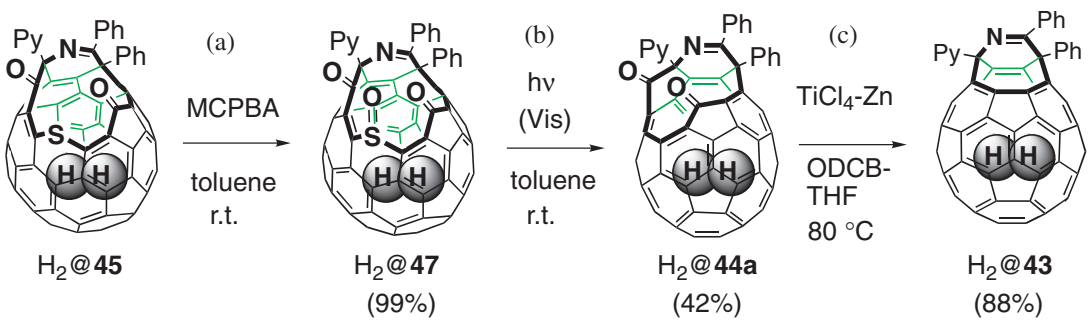

Scheme 20.

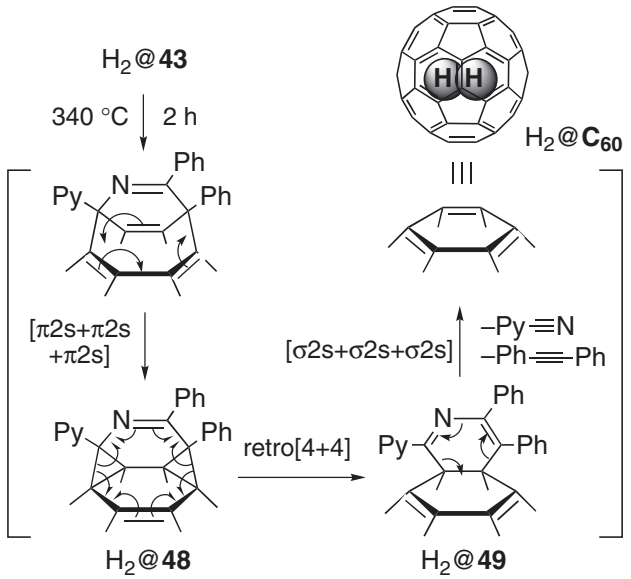

Scheme 21.

give the diene H_2@**49**. Finally, cleavage of diphenylacetylene and 2-cyanopyridine affords desired $H_2@C_{60}$. A small portion of the empty C_{60} product is assumed to have resulted from some side reaction, which might involve cleavage(s) of extra bond(s) on the cage and allowed escape of the inside hydrogen through a newly formed orifice.

The purification of $H_2@C_{60}$ was achieved by the use of recycle HPLC using a Cosmosil Buckyprep column, which has pyrene as a terminal unit connected to a silica gel support. Empty C_{60} was obtained after a total retention time of 355 min, and $H_2@C_{60}$ was obtained at the retention time of 399 min.

$H_2@C_{60}$, which was isolated as a 100% pure material, exhibited the molecular-ion peak for $C_{60}H_2$ in MALDI-TOF-MS spectrum. Thus, this molecule is a quite unusual hydrocarbon, because it does not have any C–H covalent bond. It exhibited a ^{1}H NMR signal at -1.44 ppm, which is 5.98 ppm upfield-shifted relative to the signal of dissolved free hydrogen. The extent of this upfield shift is comparable to that observed for $^3He@C_{60}$ (6.36 ppm) relative to free ^{3}He.[70] Hence, the shielding effect of the total ring currents of the C_{60} cage is supposed as nearly the same, regardless of the paramagnetic species inside the cage. The ^{13}C NMR signal of $H_2@C_{60}$ was observed at 142.844 ppm, which is 0.078 ppm downfield shifted as compared with that of empty C_{60}. The difference is so small that the electronic and/or van der Waals interaction between the fullerene π-system and the encapsulated hydrogen is considered to be quite minute. In fact, the electrochemical behavior of $H_2@C_{60}$ was found to be quite similar to that of empty C_{60} as far as three stepwise reduction waves (up to -2.0 V vs. Fc/Fc^+ in ODCB) and one oxidation peak (at $+1.62$ V in 1,1,2,2-tetrachloroethane) are concerned. When the cyclic voltammetry of $H_2@C_{60}$ was conducted at low temperature (-10 °C) under vacuum in toluene–acetonitrile (5:1), the fourth, fifth, and sixth reduction waves were found to shift slightly and gradually to more negative potentials (by 0.04, 0.07, and 0.15 V, respectively), indicating that a weak repulsive interaction might operate between hydrogen and negatively multi-charged fullerene cage.[69b]

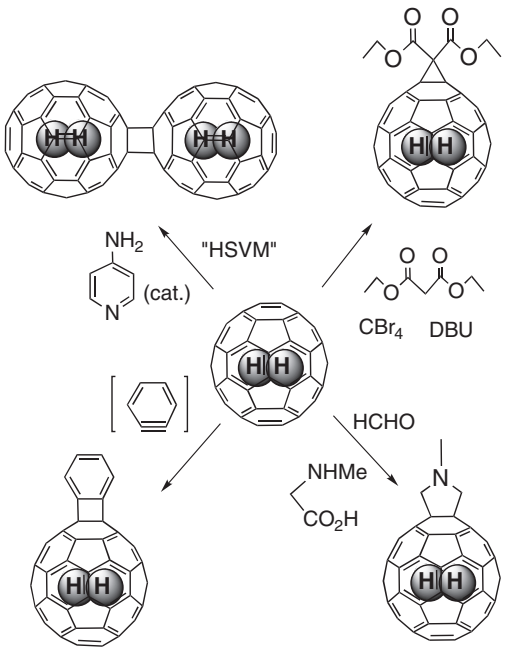

Scheme 22.

Reflecting these facts, the chemical reactivity of $H_2@C_{60}$ was found to be quite similar to that of C_{60}. As shown in Scheme 22, $H_2@C_{60}$ underwent derivatization reactions that are well known for C_{60}.[69b]

2.4 Concluding Remarks. The present work has demonstrated the possibility of synthesizing endohedral fullerene(s) not by a physical method but by the use of stepwise chemical transformations. This molecular surgical approach was shown to be effective for realization of a new endohedral fullerene, $H_2@C_{60}$. This method has an advantage that, in principle, it can be applied to the preparation of endohedral fullerenes encapsulating gas atoms or molecules with sizes comparable or smaller than a hydrogen molecule. In fact, the work has been applied to the synthesis of $H_2@C_{70}$, $D_2@C_{60}$, and $He@C_{60}$.[71]

One characteristic of the present research of the preparation of $H_2@C_{60}$ is that the behavior of hydrogen or its isotope in its entirely isolated state can be elucidated, and the physicochemical studies along this line are now under way.[72]

As an extension of the present work, the most challenging is of course to apply this method to the encapsulation of metal ions affording endohedral metallofullerenes. When they are produced in sufficiently large amounts, the investigation of their applicability to, for example, a molecular unit in electronic devices would become possible. A new era in the study of endohedral fullerenes will begin if such an event is attained. We hope that the present study is just a first step in such an ambitious attempt.

References

1 a) A. T. Balaban, M. Banciu, V. Ciorba, *Annulenes, Benzo-, Hetero-, Homo-Derivatives, and their Valence Isomers*, CRC Press, Boca Raton, **1987**. b) H. Hopf, *Classics in Hydrocarbon Chemistry*, Wiley-VCH, Weinheim, **2000**. c) Thematic Issue on

Novel Aromatic Compounds, *Tetrahedron* **2001**, *57*, Issue 17. d) Thematic Issue on Aromaticity, *Chem. Rev.* **2001**, *101*, Issue 5. e) M. Randic, *Chem. Rev.* **2003**, *103*, 3449. f) A. T. Balaban, D. C. Oniciu, A. R. Katritzky, *Chem. Rev.* **2004**, *104*, 2777. g) S. Kumaraswamy, S. S. Jalisatgi, A. J. Matzger, O. Miljani, K. P. C. Vollhardt, *Angew. Chem., Int. Ed.* **2004**, *43*, 3711, and the previous papers cited therein.

2 a) *Handbook of Organic Conductive Molecules and Polymers*, ed. by H. S. Nalwa, Wiley-VCH, Chichester, **1997**. b) *Electronic Materials: The Oligomer Approach*, ed. by K. Müllen, G. Wegner, Wiley-VCH, Weinheim, **1998**. c) *Handbook of Oligo- and Polythiophenes*, ed. by D. Fichou, Wiley-VCH, Weinheim, **1999**. d) J. M. Tour, *Acc. Chem. Res.* **2000**, *33*, 791. e) C. Joachim, J. K. Gimzewski, A. Aviram, *Nature* **2000**, *408*, 541. f) A. Nitzan, M. A. Ratner, *Science* **2003**, *300*, 1384.

3 K. Komatsu, *Bull. Chem. Soc. Jpn.* **2001**, *74*, 407.

4 K. Komatsu, T. Nishinaga, *Synlett* **2005**, 187.

5 a) L. T. Scott, M. M. Hashemi, D. T. Meyer, H. B. Warren, *J. Am. Chem. Soc.* **1991**, *113*, 7082. b) L. T. Scott, *Pure Appl. Chem.* **1996**, *68*, 291. c) L. T. Scott, P.-C. Cheng, M. M. Hashemi, M. S. Bratcher, D. T. Meyer, H. B. Warren, *J. Am. Chem. Soc.* **1997**, *119*, 10963.

6 P. W. Rabideau, A. Sygula, *Acc. Chem. Res.* **1996**, *29*, 235.

7 J. Lu, D. M. Ho, N. J. Vogelaar, C. M. Craml, R. A. Pascal, Jr., *J. Am. Chem. Soc.* **2004**, *126*, 11168.

8 a) H. W. Kroto, J. R. Heath, S. C. O'Brien, R. F. Curl, R. E. Smalley, *Nature* **1985**, *318*, 162. b) W. Krätschmer, L. D. Lamb, K. Fostiropoulos, D. R. Huffman, *Nature* **1990**, *347*, 354.

9 a) A. Hirsch, *The Chemistry of the Fullerenes*, G. Thieme Verlag, Stuttgart, **1994**. b) A. Hirsch, M. Brettreich, *Fullerenes, Chemistry and Reactions*, Wiley-VCH Verlag, Weinheim, **2005**. c) R. Taylor, *Lecture Notes on Fullerene Chemistry*, Imperial College Press, London, **1999**.

10 K. Komatsu, Y. Jinbu, G. R. Gillette, R. West, *Chem. Lett.* **1988**, 2029.

11 A. Matsuura, T. Nishinaga, K. Komatsu, *Tetrahedron Lett.* **1999**, *40*, 123.

12 A. Matsuura, T. Nishinaga, K. Komatsu, *Tetrahedron Lett.* **1997**, *38*, 3427.

13 T. Nishinaga, R. Inoue, A. Matsuura, K. Komatsu, *Org. Lett.* **2002**, *4*, 4117.

14 A. Matsuura, T. Nishinaga, K. Komatsu, *Tetrahedron Lett.* **1997**, *38*, 4125.

15 T. Nishinaga, R. Inoue, A. Matsuura, K. Komatsu, *Org. Lett.* **2002**, *4*, 1435.

16 For their spectra and theoretical interpretation, see: S. F. Nelsen, M. N. Weaver, D. Yamazaki, K. Komatsu, R. Rathore, T. Bally, *J. Phys. Chem. A* **2007**, *111*, 1667.

17 A. Matsuura, T. Nishinaga, K. Komatsu, *J. Am. Chem. Soc.* **2000**, *122*, 10007.

18 The similar change in the σ-bond length has been observed upon one-electron oxidation of adamantylideneadamantane and sesquihomoadamantane: R. Rathore, S. V. Lindeman, C.-J. Zhu, T. Mori, P. v. R. Schleyer, J. K. Kochi, *J. Org. Chem.* **2002**, *67*, 5106.

19 a) K. Komatsu, H. Akamatsu, Y. Jinbu, K. Okamoto, *J. Am. Chem. Soc.* **1988**, *110*, 633. b) K. Komatsu, H. Akamatsu, S. Aonuma, Y. Jinbu, N. Maekawa, K. Takeuchi, *Tetrahedron* **1991**, *47*, 6951.

20 a) T. Nishinaga, Y. Izukawa, K. Komatsu, *J. Am. Chem. Soc.* **2000**, *122*, 9312. b) T. Nishinaga, Y. Izukawa, K. Komatsu, *Tetrahedron* **2001**, *57*, 3645.

21 S. Ishida, T. Nishinaga, R. West, K. Komatsu, *Chem. Commun.* **2005**, 778.

22 T. Nishinaga, D. Yamazaki, H. Stahr, A. Wakamiya, K. Komatsu, *J. Am. Chem. Soc.* **2003**, *125*, 7324.

23 T. Kitagawa, K. Ogawa, K. Komatsu, *J. Am. Chem. Soc.* **2004**, *126*, 9930.

24 a) H. Sitzmann, R. Boese, *Angew. Chem., Int. Ed. Engl.* **1991**, *30*, 971. b) H. Sitzmann, H. Bock, R. Boese, T. Dezember, Z. Havlas, W. Kaim, M. Moscherosch, L. Zanathy, *J. Am. Chem. Soc.* **1993**, *115*, 12003.

25 A. Wakamiya, T. Nishinaga, K. Komatsu, *Chem. Commun.* **2002**, 1192.

26 J. Nakayama, K. Kuroda, *J. Am. Chem. Soc.* **1993**, *115*, 4612.

27 A. Wakamiya, T. Nishinaga, K. Komatsu, *J. Am. Chem. Soc.* **2002**, *124*, 15038.

28 G. Klar, in *Methoden Organische Chemie* (Houben-Weyl), ed. by E. Schaumann, Thieme, Stuttgart, **1997**, Vol. E9a, pp. 250–407.

29 a) J. Nakayama, H. Motoyama, H. Machida, M. Shimomura, M. Hoshino, *Heterocycles* **1984**, *22*, 1527. b) J. Nakayama, K. S. Choi, S. Yamaoka, M. Hoshino, *Heterocycles* **1989**, *29*, 391.

30 T. Nishinaga, A. Wakamiya, K. Komatsu, *Tetrahedron Lett.* **1999**, *40*, 4375.

31 P. D. Sullivan, *J. Am. Chem. Soc.* **1968**, *90*, 3618.

32 For recent reviews: a) S. Hotta, in *Handbook of Organic Conductive Molecules and Polymers*, ed. by H. S. Nalwa, Wiley, Chichester, **1997**, Vol. 2, Chap. 8. b) P. Bäuerle, in *Electronic Materials: The Oligomeric Approach*, ed. by K. Müllen, G. Wegner, Wiley-VCH, Weinheim, **1998**, Chap. 2. c) *Handbook of Oligo- and Polythiophenes*, ed. by D. Fichou, Wiley-VCH, Weinheim, **1999**. d) T. Otsubo, Y. Aso, K. Takimiya, *Bull. Chem. Soc. Jpn.* **2001**, *74*, 1789.

33 a) J. L. Brédas, G. B. Street, *Acc. Chem. Res.* **1985**, *18*, 309. b) A. J. Heeger, S. Kivelson, J. R. Schrieffer, W.-P. Su, *Rev. Mod. Phys.* **1988**, *60*, 781.

34 a) M. G. Hill, K. R. Mann, L. L. Miller, J.-F. Penneau, *J. Am. Chem. Soc.* **1992**, *114*, 2728. b) M. G. Hill, J.-F. Penneau, B. Zinger, K. R. Mann, L. L. Miller, *Chem. Mater.* **1992**, *4*, 1106.

35 A. Wakamiya, D. Yamazaki, T. Nishinaga, T. Kitagawa, K. Komatsu, *J. Org. Chem.* **2003**, *68*, 8305.

36 P. Bäuerle, *Adv. Mater.* **1992**, *4*, 102.

37 T. Nishinaga, A. Wakamiya, D. Yamazaki, K. Komatsu, *J. Am. Chem. Soc.* **2004**, *126*, 3163.

38 D. Yamazaki, T. Nishinaga, N. Tanino, K. Komatsu, *J. Am. Chem. Soc.* **2006**, *128*, 14470.

39 K. Komatsu, H. Akamatsu, K. Okamoto, *Tetrahedron Lett.* **1987**, *28*, 5889.

40 N. L. Frank, K. K. Baldridge, J. S. Siegel, *J. Am. Chem. Soc.* **1995**, *117*, 2102.

41 H.-B. Bürgi, K. K. Baldridge, K. Hardcastle, N. L. Frank, P. Gantzel, J. S. Siegel, J. Ziller, *Angew. Chem., Int. Ed. Engl.* **1995**, *34*, 1454.

42 F. T. Bond, H. L. Jones, L. Scerbo, *Org. Photochem. Synth.* **1971**, *1*, 33.

43 A. Matsuura, K. Komatsu, *J. Am. Chem. Soc.* **2001**, *123*, 1768.

44 T. Uto, T. Nishinaga, A. Matsuura, R. Inoue, K. Komatsu, *J. Am. Chem. Soc.* **2005**, *127*, 10162.

45 C. P. Brock, J. D. Dunitz, *Acta Crystallogr., Sect. B* **1982**, *38*, 2218.

46 a) J. Kruszewski, T. M. Krygowski, *Tetrahedron Lett.* **1972**, *13*, 3839. b) T. M. Krygowski, *J. Chem. Inf. Comput. Sci.* **1993**, *33*, 70.
47 P. v. R. Schleyer, C. Maerker, A. Dransfeld, H. Jiao, N. v. E. Hommes, *J. Am. Chem. Soc.* **1996**, *118*, 6317.
48 K. K. Baldridge, J. S. Siegel, *J. Am. Chem. Soc.* **2001**, *123*, 1755.
49 a) R. L. Soulen, S. K. Choi, J. D. Park, *J. Fluorine Chem.* **1973**, *3*, 141. b) F. W. B. Einstein, A. C. Willis, W. R. Cullen, R. L. Soulen, *J. Chem. Soc., Chem. Commun.* **1981**, 526. c) W. E. Britton, J. P. Ferraris, R. L. Soulen, *J. Am. Chem. Soc.* **1982**, *104*, 5322.
50 I. Willner, M. Rabinovitz, *J. Org. Chem.* **1980**, *45*, 1628.
51 X.-M. Wang, X.-L. Hou, Z.-Y. Zhou, T. C. W. Mak, H. N. C. Wong, *J. Org. Chem.* **1993**, *58*, 7498.
52 a) K. Komatsu, T. Nishinaga, S. Aonuma, C. Hirosawa, K. Takeuchi, H. J. Lindner, J. Richter, *Tetrahedron Lett.* **1991**, *32*, 6767. b) T. Nishinaga, K. Komatsu, N. Sugita, H. J. Lindner, J. Richter, *J. Am. Chem. Soc.* **1993**, *115*, 11642.
53 T. Nishinaga, T. Uto, K. Komatsu, *Org. Lett.* **2004**, *6*, 4611.
54 a) S. Kobayashi, S. Mori, S. Iida, H. Ando, T. Takenobu, Y. Taguchi, A. Fujiwara, A. Taninaka, H. Shinohara, Y. Iwasa, *J. Am. Chem. Soc.* **2003**, *125*, 8116. b) H. Kato, Y. Kanazawa, M. Okumura, A. Taninaka, T. Yokawa, H. Shinohara, *J. Am. Chem. Soc.* **2003**, *125*, 4391. c) É. Tóth, R. D. Bolskar, A. Borel, G. González, L. Helm, A. E. Merbach, B. Sitharaman, L. J. Wilson, *J. Am. Chem. Soc.* **2005**, *127*, 799.
55 a) H. Shinohara, *Rep. Prog. Phys.* **2000**, *63*, 843. b) S. Liu, S. Sun, *J. Organomet. Chem.* **2000**, *599*, 74. c) H. Shinohara, in *Fullerenes: Chemistry, Physics and Technology*, ed. by K. M. Kadish, R. S. Ruoff, Wiley-VCH, Weinheim, **2000**, pp. 357–393. d) *Endofullerenes: A New Family of Carbon Clusters*, ed. by T. Akasaka, S. Nagase, Kluwer Academic Publishers, Dordrecht, **2002**.
56 Y. Rubin, T. Jarrosson, G.-W. Wang, M. D. Bartberger, K. N. Houk, G. Schick, M. Saunders, R. J. Cross, *Angew. Chem., Int. Ed.* **2001**, *40*, 1543.
57 Y. Rubin, *Top. Curr. Chem.* **1999**, *199*, 67.
58 J. C. Hummelen, M. Prato, F. Wudl, *J. Am. Chem. Soc.* **1995**, *117*, 7003.
59 M. Keshavarz-K, B. Knight, G. Srdanov, F. Wudl, *J. Am. Chem. Soc.* **1995**, *117*, 11371.
60 G.-W. Wang, K. Komatsu, Y. Murata, M. Shiro, *Nature* **1997**, *387*, 583.
61 a) Y. Murata, M. Murata, K. Komatsu, *J. Org. Chem.* **2001**, *66*, 8187. b) Y. Murata, M. Suzuki, K. Komatsu, *Chem. Commun.* **2001**, 2338. c) Y. Murata, M. Suzuki, Y. Rubin, K. Komatsu, *Bull. Chem. Soc. Jpn.* **2003**, *76*, 1669.
62 Y. Murata, N. Kato, K. Komatsu, *J. Org. Chem.* **2001**, *66*, 7235.
63 Y. Murata, M. Murata, K. Komatsu, *Chem. Eur. J.* **2003**, *9*, 1600.
64 E. Allard, L. Riviere, J. Delaunary, D. Dubois, J. Cousseau, *Tetrahedron Lett.* **1999**, *40*, 7223.
65 S.-C. Chuang, Y. Murata, M. Murata, S. Mori, S. Maeda, F. Tanabe, K. Komatsu, *Chem. Commun.* **2007**, 1278.
66 Y. Murata, M. Murata, K. Komatsu, *J. Am. Chem. Soc.* **2003**, *125*, 7152.
67 H. Sawa, Y. Wakabayashi, Y. Murata, M. Murata, K. Komatsu, *Angew. Chem., Int. Ed.* **2005**, *44*, 1981.
68 J. E. McMurry, *Chem. Rev.* **1989**, *89*, 1513.
69 a) K. Komatsu, M. Murata, Y. Murata, *Science* **2005**, *307*, 238. b) M. Murata, Y. Murata, K. Komatsu, *J. Am. Chem. Soc.* **2006**, *128*, 8024.
70 a) M. Saunders, R. J. Cross, H. A. Jiménez-Vázquez, R. Shimshi, A. Khong, *Science* **1996**, *271*, 1693. b) M. Saunders, H. A. Jiménez-Vázquez, R. J. Cross, S. Mroczkowski, D. I. Freedberg, F. A. L. Anet, *Nature* **1994**, *367*, 256.
71 Y. Murata, M. Murata, S. Maeda, F. Tanabe, K. Komatsu, unpublished results.
72 For example: E. Sartori, M. Ruzzi, N. J. Turro, J. D. Decatur, D. C. Doetschman, R. G. Lawler, A. L. Buchachenko, Y. Murata, K. Komatsu, *J. Am. Chem. Soc.* **2006**, *128*, 14752.

Koichi Komatsu was born in Kyoto and received his B.Sc. from Kyoto University in 1966. In graduate school at Kyoto University, he studied the mechanism of one-electron reduction of carbocations, and obtained the Ph.D. degree. After postdoctoral study on polyquinocycloalkanes with Professor Robert West at the University of Wisconsin in 1975–76, he returned to Department of Hydrocarbon Chemistry of Kyoto University and served as Assistant Professor, Lecturer, and Associate Professor. In 1993, he moved to Institute for Chemical Research of Kyoto University and worked as Professor from 1995 to 2006, when he became Professor Emeritus of Kyoto University and moved to Fukui University of Technology as Professor of Chemistry. He received the Divisional Award of the Chemical Society of Japan (organic chemistry) in 1998, Alexander von Humboldt Research Award in 2002, Nozoe Lectureship (ISNA-11) in 2005, and the Chemical Society of Japan Award for 2005.